Agrociencia Uruguay 2022 | Volume 26 | Number NE1 | Article 799
DOI: 10.31285/AGRO.26.799
ISSN 2730-5066

Número especial en homenaje al Prof. Jorge Bossi (1934-2020)

Marine deposits of the Chuy Formation (Late Pleistocene) and isostatic readjustments in the area of Laguna de Rocha (Uruguay)

Depósitos marinos de la Formación Chuy (pleistoceno tardío) y reajustes isostáticos en el área de la Laguna de Rocha (Uruguay)

Depósitos marinhos da Formação Chuy (Pleistoceno tardio) e reajustes isostáticos na área da Laguna de Rocha (Uruguai)

Castiglioni, E.[1]; Gaucher, C.[1 2]; Perillo, G. M. E.[3]; Sial, A. N.[4]

[1]*Universidad de la República, Facultad de Ciencias, Montevideo, Uruguay*
[2]*Universidad de la República, Centro Universitario Regional Este (CURE), Polo de Desarrollo Universitario "Geología y Recursos Minerales, Treinta y Tres, Uruguay*
[3]*Universidad Nacional del Sur, Instituto Argentino de Oceanografía (CONICET-UNS), Departamento de Geología, Bahía Blanca, Argentina*
[4]*Universidade Federal de Pernambuco, NEG–LABISE, Departamento de Geologia, Recife, Brazil*

Editor
Antonella Celio
Universidad de la República, Facultad de Agronomía, Montevideo, Uruguay

Received *26 May 2021*
Accepted *30 May 2022*
Published *27 May 2022*

Correspondence
Eduardo Castiglioni,
educasti6@gmail.com

Abstract

The Chuy Formation is characterized by up to 135 m of an alternation of green pelites and fine to coarse sandstones with sparse invertebrate fossils. The marine deposits are interbedded with continental, loessic deposits of the Libertad Formation and overlain by the Dolores Formation, made up of mudstones with calcareous concretions.

The results of the radiocarbon dating showed calibrated ages of 13.9±0.2, 41.5±1.9 and 50±3 ka BP on bioclasts of marine fossils at an elevation (above sea level, asl) of -2.8, -6.13 and -8 m respectively. Such ages and elevations are in disagreement with the sea-level evolution inferred for the Late Pleistocene. Two possible explanations are: (a) the ages represent minimum ages and deposition took place during the last interglacial at 115-130 ka (Marine Isotope Stage MIS 5e), or (b) they represent depositional ages but the area experimented large isostatic readjustments during and after the last glaciation. Several lines of evidence suggest a Late Pleistocene age for the upper Chuy Formation, including the $\delta^{18}O$ curve obtained from invertebrate shells, which shows large secular variations consistent with MIS 1 to 7.

The proposed scenario envisages significant subsidence between 50-20 ka due to the far-field effects of glacial load in the Andes/Patagonia. At 20 ka the eustatic regression outpaced subsidence, leading to continentalization of the Laguna de Rocha area. Marine conditions returned at 15 ka and into the Holocene, except for continental deposits (Dolores Formation) at ca. 11-10 ka (Younger Dryas). An uplift of 115 m took place between 15 and 9 ka in the area, which is interpreted as post-glacial rebound. In the Holocene, moderate subsidence was further recorded. A regional trend is observed, with uplift of marine deposits increasing towards the W-SW, which is consistent with an explanation as post-glacial isostatic rebound.

Keywords: quaternary, glaciations, isostasy, sea-level, oxygen isotopes

Castiglioni E, Gaucher C, Perillo GME, Sial AN. Marine deposits of the Chuy Formation (Late Pleistocene) and isostatic readjustments in the area of Laguna de Rocha (Uruguay). Agrociencia Uruguay [Internet]. 2022 [cited dd mmm yyyy];26(NE1):e799. doi:10.31285/AGRO.26.799.

Resumen

La Formación Chuy se caracteriza por hasta 135 m de una alternancia de pelitas verdes y areniscas finas a gruesas con fósiles de invertebrados marinos. Los depósitos marinos están intercalados con depósitos loéssicos continentales de la Formación Libertad y sobreyacidos por la Formación Dolores, con lodolitas con concreciones calcáreas.

Los resultados de dataciones radiocarbónicas mostraron edades calibradas de 13900±200, 41500±1900 y 50000±3000 años AP, para bioclastos de fósiles marinos a una cota sobre el nivel medio del mar (NMM) de -2,8, -6,13 y -8 m, respectivamente. Estas edades y cotas están en desacuerdo con la evolución del nivel medio del mar aceptada para el Pleistoceno tardío. Dos posibles explicaciones son: (a) las edades representan edades mínimas y la depositación tuvo lugar durante el último interglacial (115-130 ka; MIS 5e), o (b) representan edades de depositación, pero el área experimentó grandes reajustes isostáticos durante y después de la última glaciación. Varias líneas de evidencia favorecen una edad Pleistoceno tardío para la Formación Chuy superior, incluyendo la curva de $\delta^{18}O$ obtenida para conchillas de invertebrados, que muestra grandes variaciones seculares consistentes con los estadios MIS 1 a MIS 7.

El escenario propuesto prevé un hundimiento significativo entre 50-20 ka debido a los efectos lejanos de la carga glacial en los Andes/Patagonia. A los 20 ka, la regresión eustática superó al hundimiento, lo que llevó a la continentalización en el área de Laguna de Rocha. Las condiciones marinas regresaron a los 15 ka y durante el Holoceno, excepto por depósitos continentales (Formación Dolores) en 11-10 ka (*Younger Dryas*). Se produjo un levantamiento de unos 115 m entre 15 y 9 ka en la zona, lo que se interpreta como un rebote post-glacial. En el Holoceno, se registra nuevamente un hundimiento moderado. Se observa una tendencia regional, con un aumento de los depósitos marinos hacia el W-SW, lo que es consistente con un rebote isostático post-glacial.

Palabras clave: cuaternario, glaciaciones, isostasia, nivel del mar, isótopos de oxígeno

Resumo

A Formação Chuy é caracterizada por uma alternância de até 135 m de folhelhos verdes e arenitos finos a grossos com fósseis de invertebrados marinhos. Depósitos marinhos estão intercalados com depósitos loessicos continentais da Formação Libertad é recobertos pela Formação Dolores, com lamitos com concreções calcárias

Os resultados da datação por radiocarbono mostraram idades calibradas de 13.900±200, 41.500±1.900 e 50.000±3.000 anos AP, para bioclastos de fósseis marinhos em uma elevação acima do nível médio do mar de -2,8, -6,13 e -8 m, respectivamente. Essas idades e alturas estão em desacordo com a evolução do nível do mar aceita para o final do Pleistoceno. Duas explicações possíveis são: (a) as idades representam as idades mínimas e a depositação ocorreu durante o último período interglacial (115-130 ka; MIS 5e), ou (b) representam as idades de depositação, mas a área experimentou grandes reajustes isostáticos durante e após a última glaciação. Várias linhas de evidência favorecem uma idade do Pleistoceno tardio para a Formação Chuy superior, incluindo a curva do $\delta^{18}O$ obtida para conchas de invertebrados, que mostra grandes variações seculares consistentes com estágios MIS 1 a MIS 7.

O cenário proposto prevê uma subsidência significativa entre 50-20 ka devido aos efeitos distantes da carga glacial nos Andes/Patagônia. Aos 20 ka, a regressão eustática superou a subsidência, levando à continentalização na área da Laguna de Rocha. As condições marinhas retornaram em 15 ka e no Holoceno, exceto para depósitos continentais (Formação Dolores) em 11-10 ka (*Younger Dryas*). Uma subida de 115 m foi inferida entre 14 e 9 ka na área, o que é interpretado como um elevação pós-glacial. No Holoceno, uma subsidência moderada foi registrada novamente. Observa-se uma tendência regional, com um aumento dos depósitos marinhos em direção ao W-SW, o que é consistente com uma explicação como um rebote isostático pós-glacial.

Palavras-chave: quaternário, glaciações, isostasia, nível do mar, isótopos de oxigênio

1. Introduction

The Quaternary is characterized globally by an alternation of glacial and interglacial periods[1] that is recorded in the marine and transitional environments, as variations in the mean sea level (MSL) with amplitudes of up to 140 m[2] (Fig. 1). Most of this sea-level variation is explained by captured water in polar ice caps during glaciations and its subsequent return to the ocean during interglacial periods (glacioeustasy), as demonstrated in the study of oxygen isotope ratios ($\delta^{18}O$) in marine carbonates[3] (Fig. 1). However, at the local level, and to a lesser extent at the global level, other factors also affect sea level, such as glacio- and hydro-isostasy. In the first case, it refers to the weight of the glacial caps that relatively sink the continents, with

the best-studied example being the Scandinavian peninsula[4-5]. Hydro-isostasy, on the other hand, causes variable variations of different sign: during the glaciations, the absence of tens or hundreds of meters of water column on the shelves determines uplift movements, and the interglacials favor the relative subsidence of these basins[4][6]. Determining the causes of sea-level variations, even on tectonically stable shelves, is, therefore, a relatively complex task.

Figure 1. Sea level variation curve[23] and oxygen isotope ratios measured as variation from present-day values ($\Delta\delta^{18}O$; North Atlantic, well NA87/22-25: 3.32 ‰VPDB, Pacific, well V19-30: 3.45 ‰VPDB) over the last 150 ka[2]. The duration of the different marine isotopic stages (MIS) is indicated

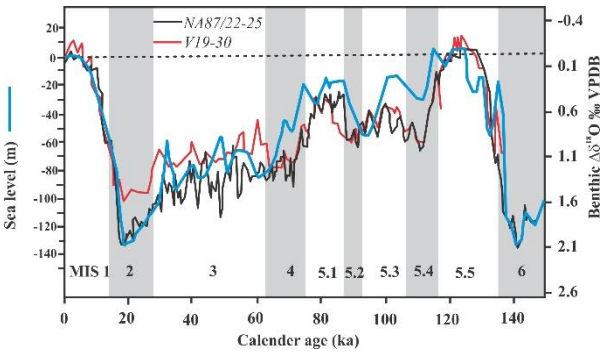

In Uruguay, sea-level reconstructions were carried out mainly for the Holocene, using regional curves as a guide in some cases, sometimes too general for the study area[7-13]. According to some studies, sea level reached 4 m approximately 6 ka ago[11][14-15]. These heights above present-day msl are consistent with the paleoshorelines of Laguna de Rocha. There are relatively few studies on the Pleistocene in Uruguay, which concentrate on the marine deposits of the Chuy Formation[16]. According to all these studies, the elevation of the marine deposits often exceeds the current MSL[17-18], as happens in Argentina[19-20], where the highest elevation of 7 m was detected in the estuary of Bahía Blanca[21], and southern Brazil. More interestingly, these deposits yielded radiocarbon ages consistently between 35 and 15 ka, when sea level was between -80 and -115 m[9][17][19], thus presenting an obvious interpretation challenge.

This article presents a geological study of the Laguna de Rocha basin, where the Chuy Formation outcrops. The lagoon is located in the SE sector of Uruguay (Fig. 2), and separated from the Atlantic Ocean by a narrow sandy bar with sporadic openings. Detailed geological mapping was carried out, along with ^{14}C datings, analysis of $\delta^{18}O$ in mollusks and descriptions of 44 wells that complement data already published[9-10][22]. Based on these new data, the possible causes of the age vs. elevation discrepancy, which is evident in the deposits of the Chuy Formation, are discussed.

Figure 2. Geological sketch map of Uruguay[24] and location of the study area shown in Fig. 3

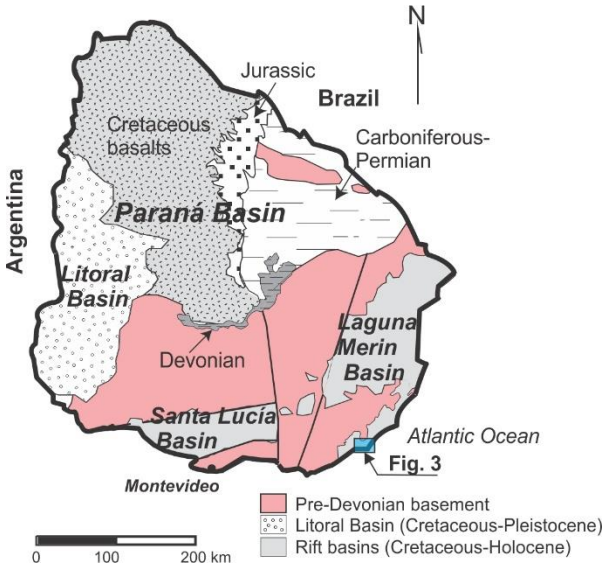

2. Geological Background

2.1 Prequaternary Regional Geology

The geological structure of the study area consists of a crystalline basement corresponding to the Cuchilla Dionisio Terrane[24](Fig. 2). The main Precambrian unit is the Rocha Formation, which is exposed mostly in the coastal strip of both the Atlantic Ocean and the Laguna de Rocha, with excellent outcrops in La Paloma and La Pedrera towns (Fig. 3). It is a low-grade metasedimentary succession of turbiditic origin, the age of which was determined as Late Ediacaran (564-543 Ma)[25]. The Formation consists of metapsammites, metapelites and metawackes arranged in thin, tabular strata (1 to 10 cm) and sporadic, thicker beds (>1 m)[26].

The area became relatively stable towards 530 Ma, after having experienced horizontal displacements of blocks along the Sierra Ballena Shear Zone, heading NNE[27] (Fig. 2). There is no record of tectonic activity between the beginning of the Cambrian and about 140 Ma (Lower Cretaceous). During that long period, the subsoil of eastern Uruguay was

part of the Gondwana supercontinent and thus remained stable[24]. After cratonization, the first detectable tectonic event is a major lava effusion (basalts, rhyolites; Fig. 2), associated with the preambles of the opening of the Atlantic Ocean, which by the Ar-Ar and K-Ar method yielded ages between 134 and 128 Ma[28-29]. In the study area, during the early Cretaceous, the opening of the Laguna Merín Basin occurred (Fig. 2), a rift associated with the Pelotas Basin[29]. From that moment until the Late Cretaceous, there was a moderate overheating up to about 70 °C in Uruguay, although not in the region of the Laguna de Rocha, where there was a continuous cooling (uplift) of the basement during the Meso- and Cenozoic period up to room temperatures[30].

2.2 Quaternary deposits

The sedimentary record of the Quaternary in the study area is composed of marine-transitional and continental interbedded or interdigitated deposits, within the framework of the Pelotas Basin[31-32] (Figs. 3-4). The marine deposits correspond to the Chuy Formation, of Late Pleistocene age, and the Villa Soriano Formation, of Holocene age[18][21]. Continental deposits include the Libertad Formation, which is interbedded with the Chuy Formation, and the Dolores Formation, which separate the Chuy and Villa Soriano formations. The two formations are characterized by mudstones representing, in part, resedimented loess[32]. Based on their fossil mammal content and ^{14}C dating available, both units are assigned to the Late Pleistocene with ages 17 to 30 ka for the Libertad Formation, and 11 ka for the Dolores Formation[18][33]. During the deposit of the continental silt-loess units, the climate was arid and cold with sparse vegetation, allowing the colluviation of the soils of the previous interglacial.

Figure 3. Geological map in scale 1:50000 made in this study, with the location of studied wells. The position of the AA' and BB' cross sections is indicated (Fig. 4)

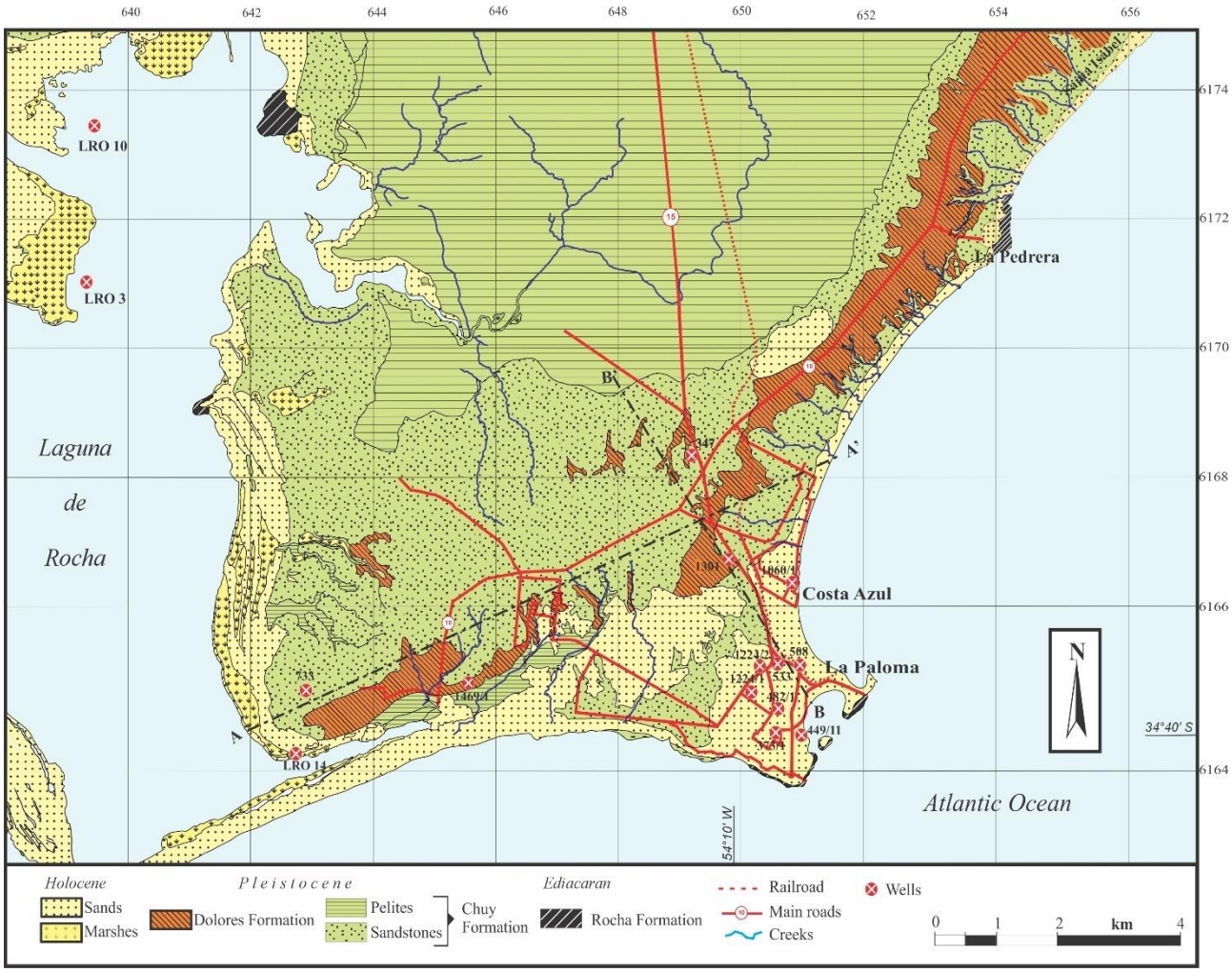

Figure 4. Geological sections AA' and BB' (see Fig. 3), showing the subsurface structure in the study area

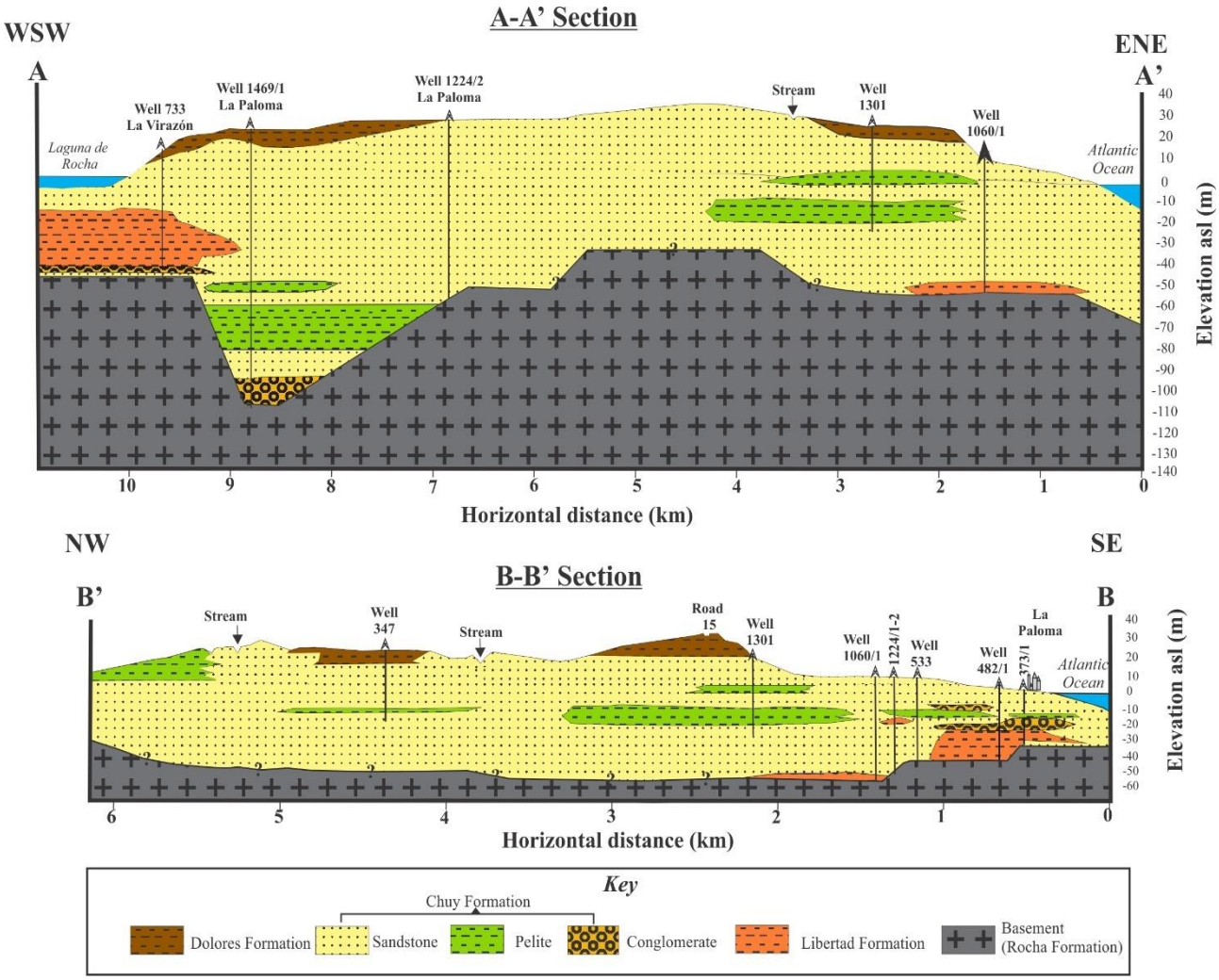

After the deposition of the last continental unit (Dolores Formation), the sea level rose during the Holocene, generating several episodic transgressions at +5, +2.5 and +2 m above the present msl with the maximum between 5 to 6 ka[7][13]. Coarse sands and gray clays were then deposited with abundant mollusks, mainly bivalves, which are included within the Villa Soriano Formation[18]. No outcrops of the Villa Soriano Formation were found in the study area, but it is mentioned here anyway since it was described in cores extracted from the Laguna de Rocha (wells LRO 10 and LRO 12, Figs. 3, 5), with ^{14}C datings between 7.2 and 4.1 ka[9-10]. In any case, it is of interest here to differentiate between the Villa Soriano Formation and the Chuy Formation, since both have a marine origin, but different ages. The different lithological characteristics and stratigraphic position allow a differential diagnosis (Table 1).

The Chuy Formation, the main unit of interest in this work, was defined by Delaney[34] and Goñi and Hoffstetter[35] as Chuy Formation. Elizalde[36] proposed to designate the sedimentites mapped as Chuy Formation with the name of Barra del Chuy Formation, integrated, at least partially, with the denominations of Paso del Puerto[37] and Chuy[38]. Bossi and collaborators proposed to call it Barra del Chuy Formation[24], based on the fact that it seems more logical to designate the unit with the name of a point of good exposure and, in addition, very close and homonymous. However, it is proposed in the present study to maintain the name of Chuy Formation, accepting the Barra del Chuy as stratotype and type area[24]. At least three transgressive episodes were identified, designated, respectively, as Chuy I (Lower Chuy), Chuy II and Chuy III[39].

Lithologically the Chuy Formation presents two main facies: fine yellowish sandstones, with variable ferrification (Fig. 6), and occasional fossil mollusks and green shales. Based on the fossil foraminifera and mollusks described from this unit, environments vary from fluviomarine to frankly marine, but in the area of the Laguna de Rocha only marine environments and predominantly normal-marine salinity are recorded[22].

Figure 5. Location of the wells with results of ^{14}C datings in bioclasts of the Chuy Formation and their elevations above msl. Selected ^{14}C ages are also indicated, made in sediment cores (LRO 3, 10 and 14) within the Laguna de Rocha[9]

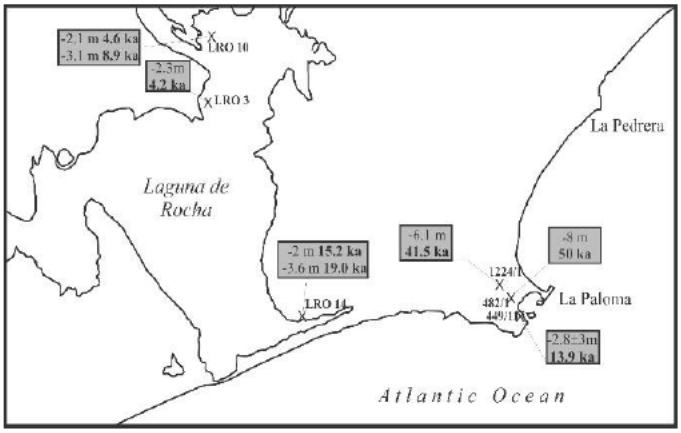

Table 1. Differential comparative lithological characteristics of the Chuy and Villa Soriano formations

Characteristic	Chuy Formation	Villa Soriano Formation
Top Contact	Dolores Fm	Current soil or dunes[18]
Occurrence elevations relative to msl	47 to -120 m in the study area	0 to 6 m Maldonado-Rocha[18][11]. Inside the Laguna de Rocha: -3.5/-5.7 m according to[10]
Lithologies	Fine-very fine sandstones, green clays	Grey clays, coarse to very fine sands[18][40]
Ferrification crusts and hematite concretions	Common and typical[18][35] also in the studied sections	No known occurrences
Abundance of bivalves	Rare, restricted to specific intervals	Abundant, typical[18]
Thickness	Up to 10 m measured in outcrop and 135 m in wells of the area	<5 m in outcrop, up to 20 m in wells[18]

3. Material and methods

3.1 Geological cartography

The presented cartography (Fig. 3) consists of a geological map of the study area scale 1:50000. Stereographic pairs of aerial photos of scale 1:20000 from the Servicio Geográfico Militar (SGM, Uruguay) taken in 1966, were used for its drawing. Additionally, data obtained from the topographic sheet "La Paloma" in scale 1:50000 of the SGM were verified and assembled in order to update the information.

3.2 Borehole sampling

Samples of boreholes carried out in the area of La Paloma were studied, which are deposited at the National Directorate of Mining and Geology (DINAMIGE by its Spanish acronym). These are found in glass jars labeled with the name of the well and arranged in variable depth jumps of between 2 to 10 m depending on the depth and the well. When the material was described, a large number of bioclasts could be found, which at some levels were a mixture of taxonomically unidentifiable material. However, it was possible to identify known species, which allowed inferences about the depositional environment, as well as the bathymetric and tidal characteristics present during their deposition.

After isolating the larger bioclasts, the remaining smaller fragments were separated using a 1 mm sieve so as to have a sufficiently large sample for further analysis of ^{14}C and determination of their isotopic values of O and C. For the study of the wells, a Zeiss SV-11 binocular stereomicroscope with digital camera was used, in order to describe the texture, mineralogy and fossils in the most detailed way possible. The elevation was calculated for each sample relative to the Wharton zero corrected over the Montevideo harbour, taking into account the depth of the sample and the elevation of the well

head, using the contour lines of the topographic chart. In some cases, there is uncertainty in the level of the well head, because it was not originally determined and because the coordinates of the well have often uncertainties of about ±250 m. The corresponding uncertainties of the elevation are indicated in these cases (Tables 2-3).

Figure 6. Photographs of outcrops and thin sections. (A) Mudstones with carbonate concretions of the Libertad Formation under- and overlain by sandstones of marine origin (Santa Isabel). (B) Contact between the Dolores Formation and the Chuy Formation in the area of Santa Isabel. (C-D) Characteristic crusts of the Chuy Formation. C shows mostly crusts of limonite, hematite and oxides of Mn, and D crusts composed mainly of hematite. (E) Microphotograph of ferrificated sandstones of the Chuy Formation, with parallel nicols. (F) Same as previous with crossed nicols. Note the plagioclase, quartz, lithic and epidote (top left) clasts, as well as abundant hematite-limonite cement

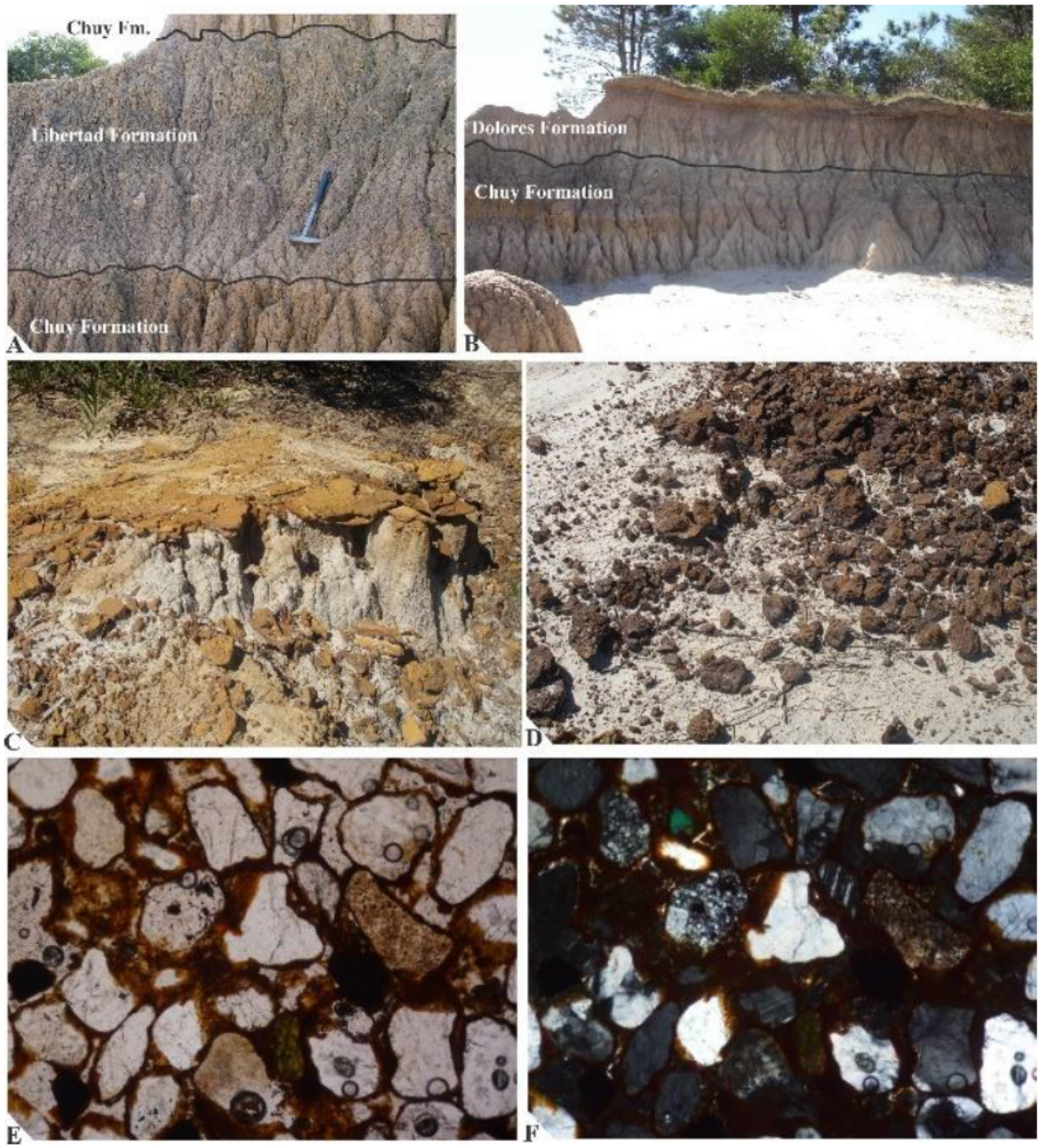

Table 2. ^{14}C datings in bivalves of the Chuy Formation

Species	Uncorrected ^{14}C years BP	Corrected to cal years BP	Method	Sample	Well	Elevation m
Various	12035 ± 110	**13900 ±200**	Traditional	E11	449/11	**-2,75±3 m**
Various	39995 ±1995	**41500 ± 1900**	Traditional	A1	1224/1	**-6,13**
Ostrea patagonica	47200 ±2900	**50000 ± 3000**	AMS	A7	482/1	**-8**

Table 3. Isotopic ratios of C and O for invertebrates of the Chuy Formation in the study area and in its type area (well 1257), measured and vital effect-corrected data ($\delta^{18}O$). The values in italics indicate that a correction could not be applied due to unknown species (undet.) or specific vital factor value

Sample	Well	$\delta^{13}C_{VPDB}$ ‰	$\delta^{18}O_{VPDB}$ ‰	$\delta^{18}O_{VPDB}$ ‰ corrected	Elevation m amsl	Species
A1	1224/1	1.53	-0.91	0.18	*-6.1*	*Ostrea* sp.
A2	1224/2	-2.92	-3.33	-2.24	-9.2	*Ostrea* sp.
A3	533/1	1.86	-1.17	-0.078	-5.8	*Ostrea* sp.
A4	508	1.39	-1.82	-0.73	-3.9	*Ostrea* sp.
A5	508	1.07	-1.84	-0.75	-6.9	*Ostrea* sp.
A6	508	0.99	-1.34	-0.25	-5.4	*Ostrea* sp.
A7	482/1	1.26	-1.15	-0.058	-8	*Ostrea* sp.
A8	482/1	-0.09	-2.11	-1.02	-0.85	*Ostrea* sp.
A16	373/1	-1.55	-3.40	-2.31	-2.5	*Ostrea* sp.
A17	482/1	1.25	-1.10	-0.01	-2.5	*Ostrea* sp.
B13	449/11	2.39	-0.94	-0.84	-1.3±3	*Brachidontes rodriguezi*
B14	449/11	2.44	-0.59	-0.48	1.8±3	*Brachidontes rodriguezi*
C9	1224/1	0.53	-1.96	-0.87	-8.1	Pectinidae
D15	373/1	-1.20	-3.67	-3.57	-8.5	*Amphybalanus* sp.
E10	449/11	3.30	0.27	0.23	-2.8±3	*Glycymeris longior*
E11	449/11	2.59	0.55	0.51	-2.8±3	*Glycymeris longior*
12	449/11	2.02	0.34	-0.75	-0.75±3	*Mactra guidoii*
1257 1-A	1257	2.68	1.18	*1.18*	-1.5	Undet.
1257 1-B	1257	1.43	0.85	*0.85*	-1.5	*Buccinanops* sp.
1257 1-C	1257	1.76	2.23	*2.23*	-1.5	Veneridae
1257 1-D	1257	0.16	3.06	*3.06*	-1.5	*Heleobia* sp.
1257 2-A	1257	0.26	0.16	*0.16*	-10.5	Veneridae
1257 3-A	1257	-4.12	-1.46	-0.37	-11.5	*Ostrea* sp.
1257 3-B	1257	1.40	-0.31	*-0.31*	-11.5	Veneridae
1257 3-C	1257	-0.99	0.02	*0.02*	-11.5	Undet.
1257 4-B	1257	-2.10	-0.72	0.37	-12.5	*Ostrea* sp.
1257 5-B	1257	-1.70	-0.99	0.10	-13.5	*Ostrea* sp.
1060 1-A	1060/1	0.82	-0.15	*-0.15*	-2.0	Undet.
1060 2-A	1060/1	1.02	-0.43	*-0.43*	-5.0	Veneridae
1060 2-B	1060/1	0.06	0.71	*0.71*	-5.0	*Corbula* sp.
1060 2-C	1060/1	0.65	0.23	*0.23*	-5.0	Undet.
1060 3-A	1060/1	0.37	0.21	*0.21*	-8.3	Undet.
1060 4-A	1060/1	1.52	-0.01	*-0.01*	-12.6	Undet.
1060 5-A	1060/1	-6.20	-2.89	*-2.89*	-21.5	Undet.

3.3 Thin sections and X-ray diffractometry

The samples of consolidated and semi-consolidated material (e.g., ferrous concretions), before cutting, were impregnated with epoxy resin (Araldite 2020®). They were then cut with a diamond saw and glued with Araldite® on petrographic slides. Subsequently, they were ground down to ca. 50 µm in a WOCO 50 thin section machine; the final polishing to 30 µm was done with 1000-mesh silicon carbide abrasive. The observation was carried out with a Leica DM LP petrographic microscope in the Laboratory of Micro-

paleontology of the Facultad de Ciencias, Universidad de la República, with a coupled digital camera Leica FC 290-HD, with quantification software LAS Phase Expert. The mineralogy of the matrix of the sandstones was determined with an X-ray diffractometer Philips PW 1729 also at the Facultad de Ciencias.

3.4 Stable isotopes

The sampling of the mollusks used for the analyses of ^{14}C and stable isotopes was done by separating them with a sieve from the sediment matrix. For bioclasts intended for the analysis of $\delta^{18}O$ and $\delta^{13}C$, a 50 mg valve fragment was isolated in each case. It was then washed with 10% H_3PO_4 so as to dissolve the outermost layer and rid it of impurities. The sample was then ground to a fine powder and approximately 20 mg were measured. These were sent in Eppendorf tubes to the LABISE *(Laboratório de Isotopos Estáveis)* of the Federal University of Pernambuco (Recife, Brazil).

CO_2 was extracted from the carbonates via a reaction with orthophosphoric acid in a high vacuum chamber at 25°C, and cryogenically purified[41]. The released gas was analyzed to determine the O and C isotopes in a double-entry, triple-collector spectrometer (VG Isotech SIRA II). For this, BSC reference gas (*Borborema Skarn Calcite*) was used, which is calibrated with reference to the standards NBS-18, NBS-19 and NBS-20, the latter with a value of $\delta^{18}O$ of -11.3‰ PDB and $\delta^{13}C$ of 8.6‰. Accuracy based on multiple comparisons against the NBS 19 standard is greater than 0.1‰ for C and O.

3.5 ^{14}C Datings

The bioclasts employed for dating were used differently according to the dating method. In the case of traditional ^{14}C datings, bioclast fragments of various species were collected in wells, 20.2 g for sample E11 and 26.5 g for sample A1. For sample A7, dated by the AMS (Accelerator Mass Spectrometry) method, 1.86 mg of a *Ostrea patagonica* valve was used.

Bioclasts used for conventional ^{14}C dating were not previously subjected to acid treatment upon shipment, since this already integrated the standard radiodating procedure. The reading of conventional ^{14}C was carried out in the Laboratorio de Datación ^{14}C of the Facultad de Química of UdelaR (Montevideo). The samples were treated with diluted HCl until the loss of 15% of the original mass, to remove contaminants and outer layers. Total organic matter was dissolved in benzene and the activity of ^{14}C was measured with a Packard Tricarb 2560 TR/XL scintillation spectrometer. Age is expressed in years ^{14}C BP uncalibrated, corrected by isotopic fractionation by normalizing the values from $\delta^{13}C$ to -25‰. Errors $\pm 1\sigma$ include uncertainties in counting statistics.

Selected samples were analyzed by the AMS method at the University of Arizona (USA), pretreated with 1% HCl at 60 ºC. CO_2 was obtained from the carbonate by a quartz tube with CuO and Ag wool at 900°C. The CO_2 obtained was reduced to graphite with H_2 at 600 °C on a 2 mg Fe catalyst. The C/Fe mixture was compressed to a tablet form for the AMS reading. The concentration of ^{14}C was measured by simultaneous comparison of the beams corresponding to ^{13}C and ^{12}C with the CO_2 of an oxalic acid standard. Then, for the measurement and calculation of age, a vertical section was used and its $\delta^{13}C$ was measured by isotopic fractionation based simultaneously on the ratios between $^{13}C/^{12}C$ con $^{14}C/^{12}C$.

4. Results

4.1 Geological Map and Cross Sections

The geological map scale 1:40000 of the study area is presented (Fig. 4). Based on this map and the descriptions of wells below, geological sections AA' and BB' were made in order to show the geological structure of the area. Intervals without data exist between some locations of the transect due to the location of the wells (Fig. 4). The lithological description of the different wells studied is described below.

4.2 Stratigraphy

In general, the stratigraphy published in regional geological charts is confirmed[24][40]. A basement composed of metasandstones and metapelites of the Rocha Formation is observed, which crops out along the coastal strip (La Paloma-La Pedrera) and inland in the Cuchilla del Rey (to the NW of the mapped area), as well as in some rocky points of the Laguna de Rocha (Fig. 3). Between these basement areas, a small graben is developed that is completely filled with Quaternary units, reaching a thickness of 140 m in the well 1469/1 (Fig. 4). The subsidence of 140 m and the thickness of the Quaternary units there are unusual in Uruguay[32], and suggest that the Laguna Merín Basin has continued its subsidence during the Quaternary, generating accommodation space[15][42]. The basin with filling of mainly Quaternary age that develops in the study area is called here La Paloma Graben[43].

The Quaternary succession is composed of an alternation between marine sandstones and pelites of the Chuy Formation and at least two horizons of mudstones of continental origin, from base to top: Libertad Formation and Dolores Formation (Fig. 4).

4.2.1 Chuy Formation

An alternation is observed in the profiles in the study area (Figs. 7-12) from clays to coarse sandstones and conglomerates. The pelitic levels, apparently more frequent at the base, may have scattered sand and gravel of different shades from green to greyish green, with frequent mottles from rust-red to yellowish tones, predominant in the upper part.

Figure 7. Stratigraphic column of the 1469/1 well. Coordinates (x, y) relative to the Datum Yacaré and the elevation (z) relative to the Wharton zero. Dol: Dolores Formation

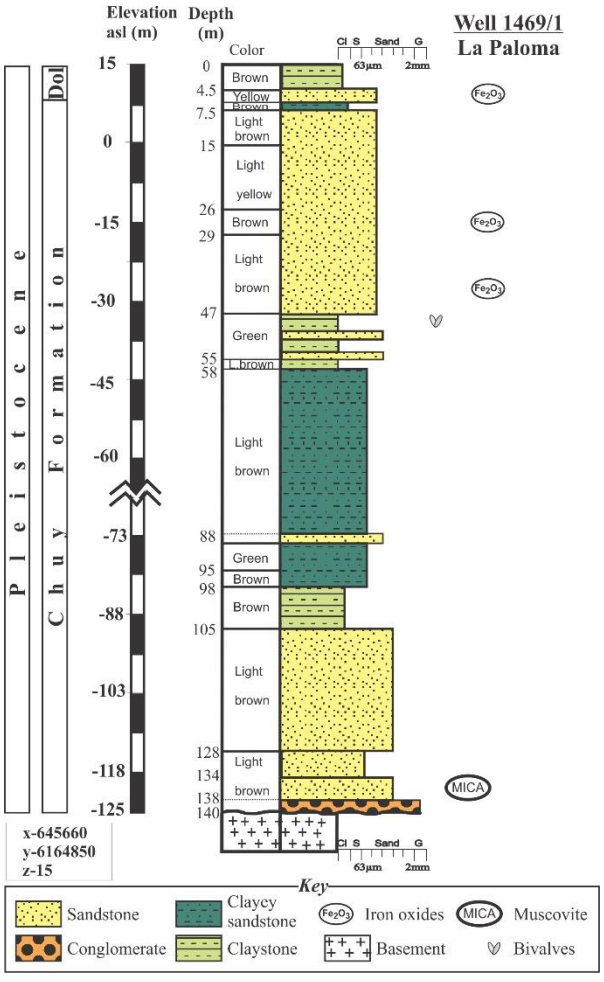

Sandstones are fine to medium-grained, rarely coarse, predominantly subarkose and quartz sandstone, with a relatively high proportion of dense minerals. The strata are solid, 0.5 to 2 m thick. The yellowish and reddish-yellowish colors are the most frequent; centimetric ferruginous crusts occur in this unit (Fig. 6) in up to four levels in the same profile. Iron oxides and calcium carbonate concretions are found at the top levels. These occasionally present ferruginous nodules with dense minerals: zircon, tourmaline, biotite, rutile, garnet, andalusite, hornblende, epidote, actinolite and grains occasionally covered by a ferruginous film (Fig. 6). By means of X-ray diffractometry, illite was determined in the clay fraction of the sandstones, which may come from the alteration of the feldspathic clasts and/or the scarce matrix.

Figure 8. Stratigraphic column of the 733 well. Coordinates (x, y) relative to the Datum Yacaré and the elevation (z) relative to the Wharton zero. Dol: Dolores Formation

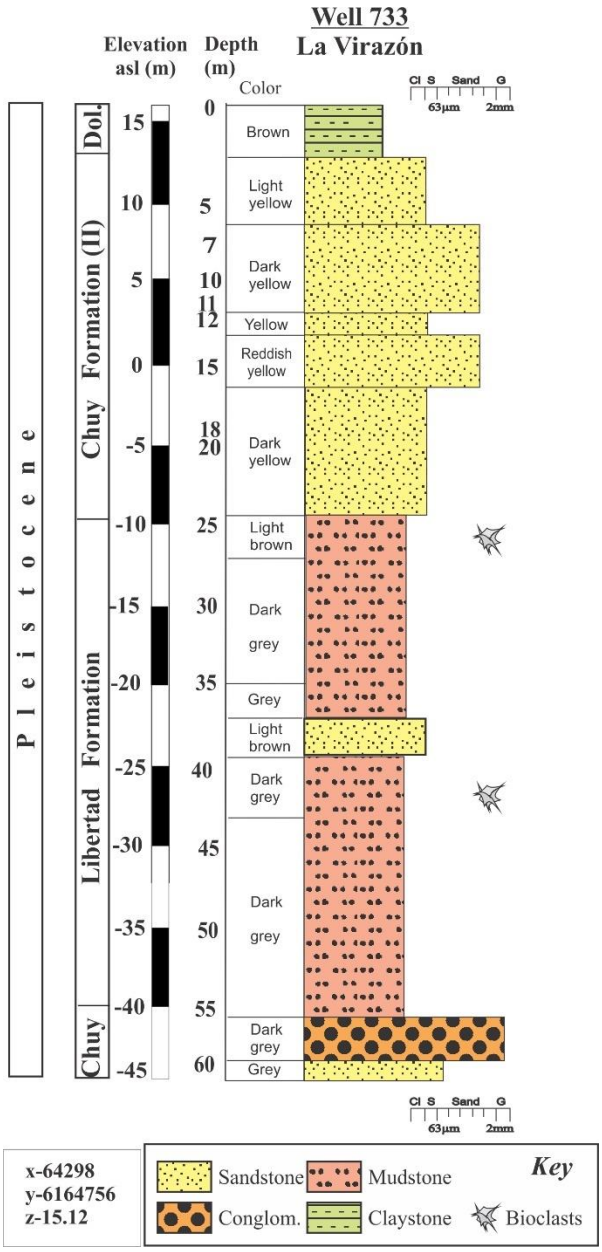

Figure 9. Stratigraphic column of well 449/1 with data of $\delta^{18}O$, $\delta^{13}C$ and ^{14}C dating (in cal years BP) in mollusks. Coordinates (x, y) relative to the Datum Yacaré and the elevation (z) relative to the Wharton zero

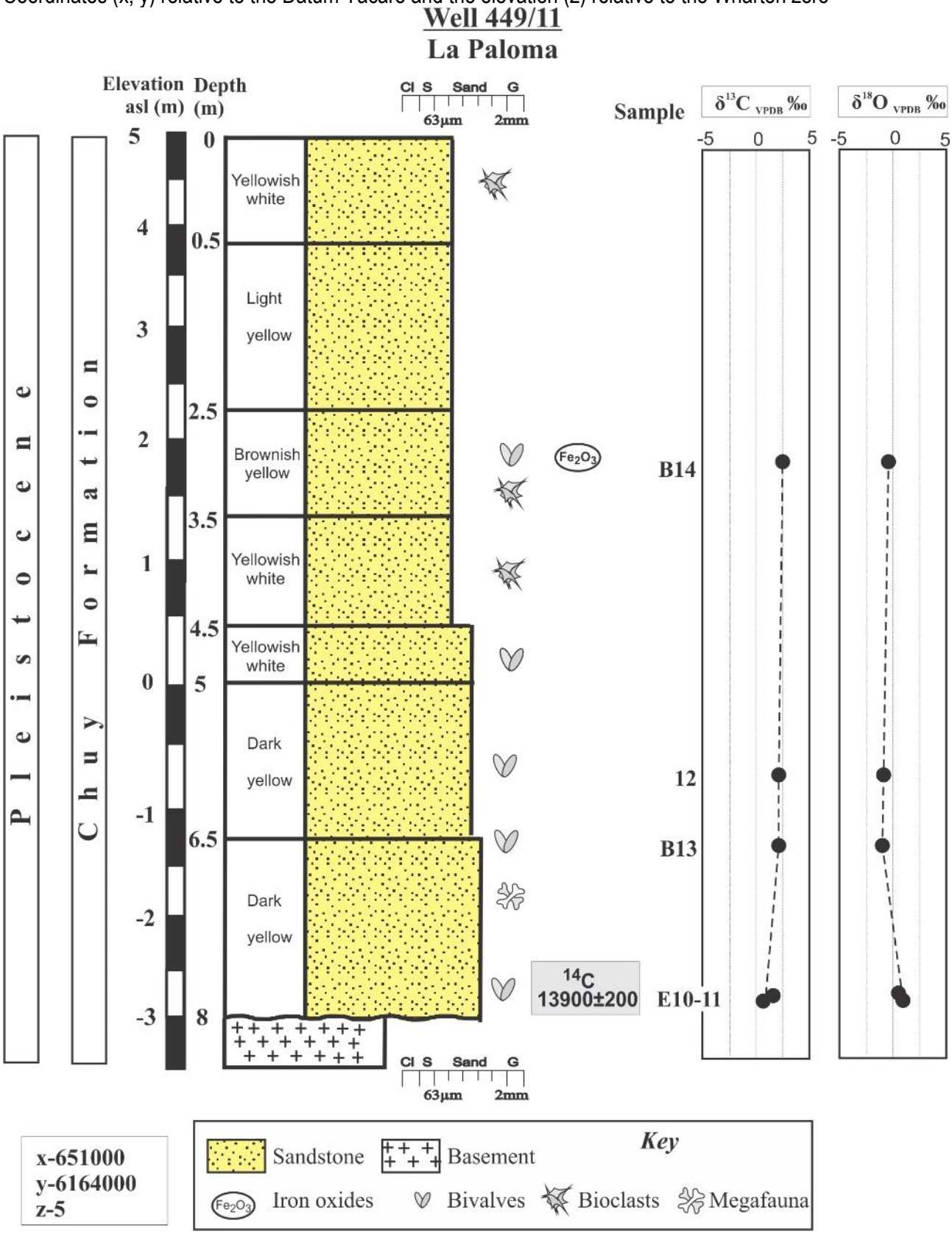

Figure 10. Stratigraphic column of well 1224/1 with data of $\delta^{18}O$, $\delta^{13}C$ and ^{14}C dating (in cal years BP) in mollusks. Coordinates (x, y) relative to the Datum Yacaré and the elevation (z) relative to the Wharton zero

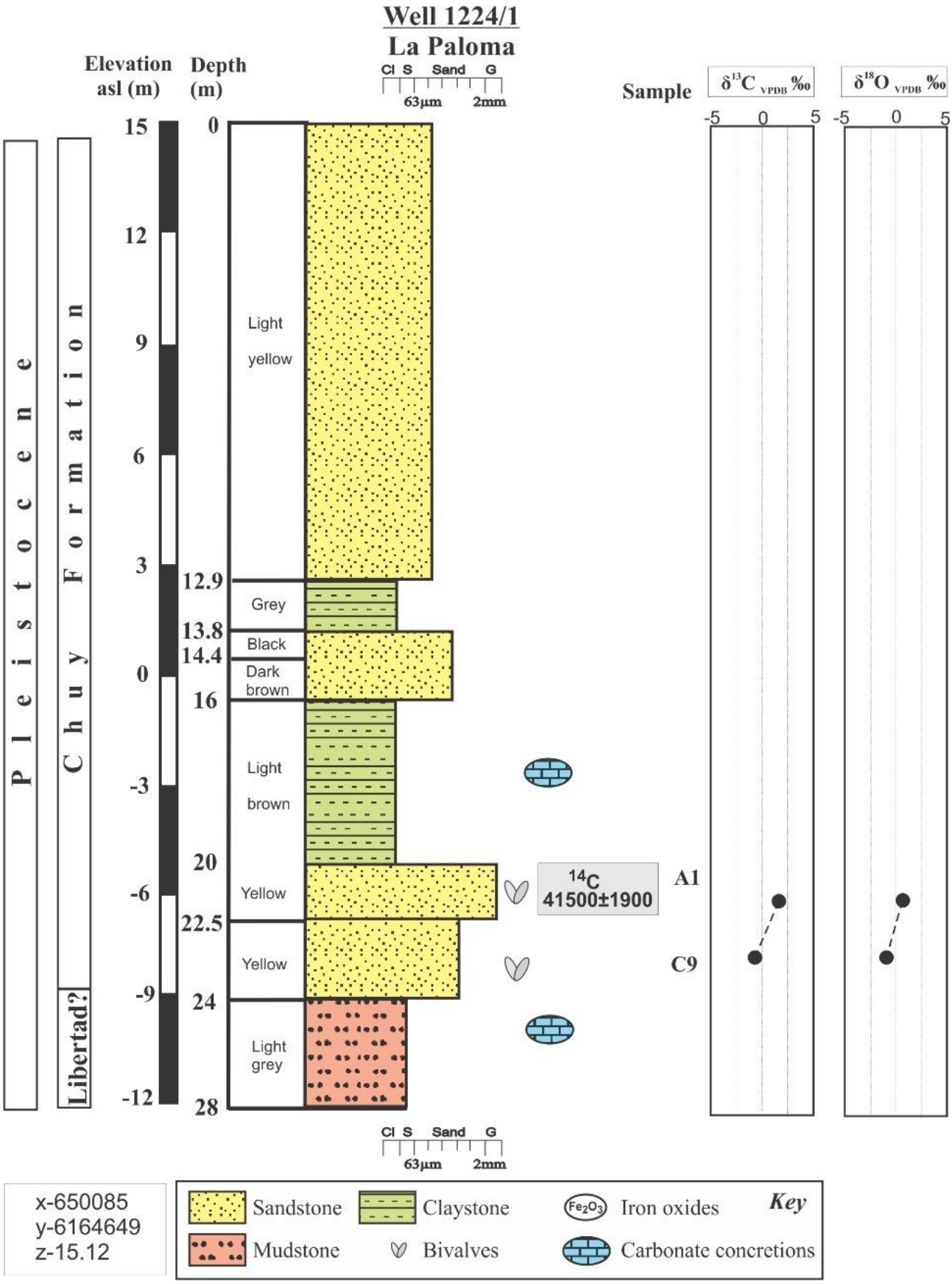

Figure 11. Stratigraphic column of well 482/1 with data of $\delta^{18}O$, $\delta^{13}C$ and ^{14}C dating (in cal years BP) in mollusks. Coordinates (x, y) relative to the Datum Yacaré and the elevation (z) relative to the Wharton zero

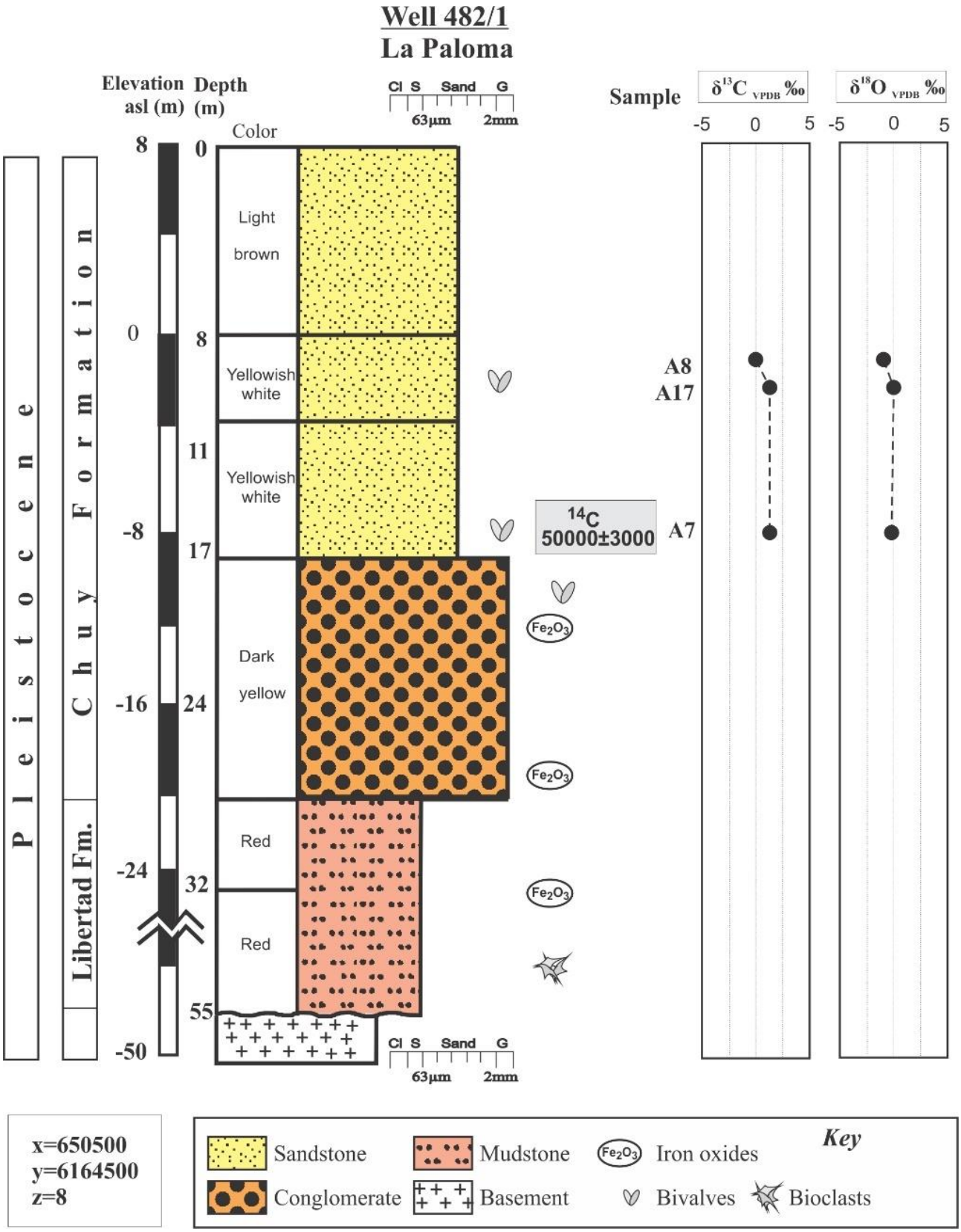

Figure 12. Stratigraphic column of well 508 with data of $\delta^{18}O$, $\delta^{13}C$ and ^{14}C dating (in cal years BP) in mollusks. Coordinates (x, y) relative to the Datum Yacaré and the elevation (z) relative to the Wharton zero

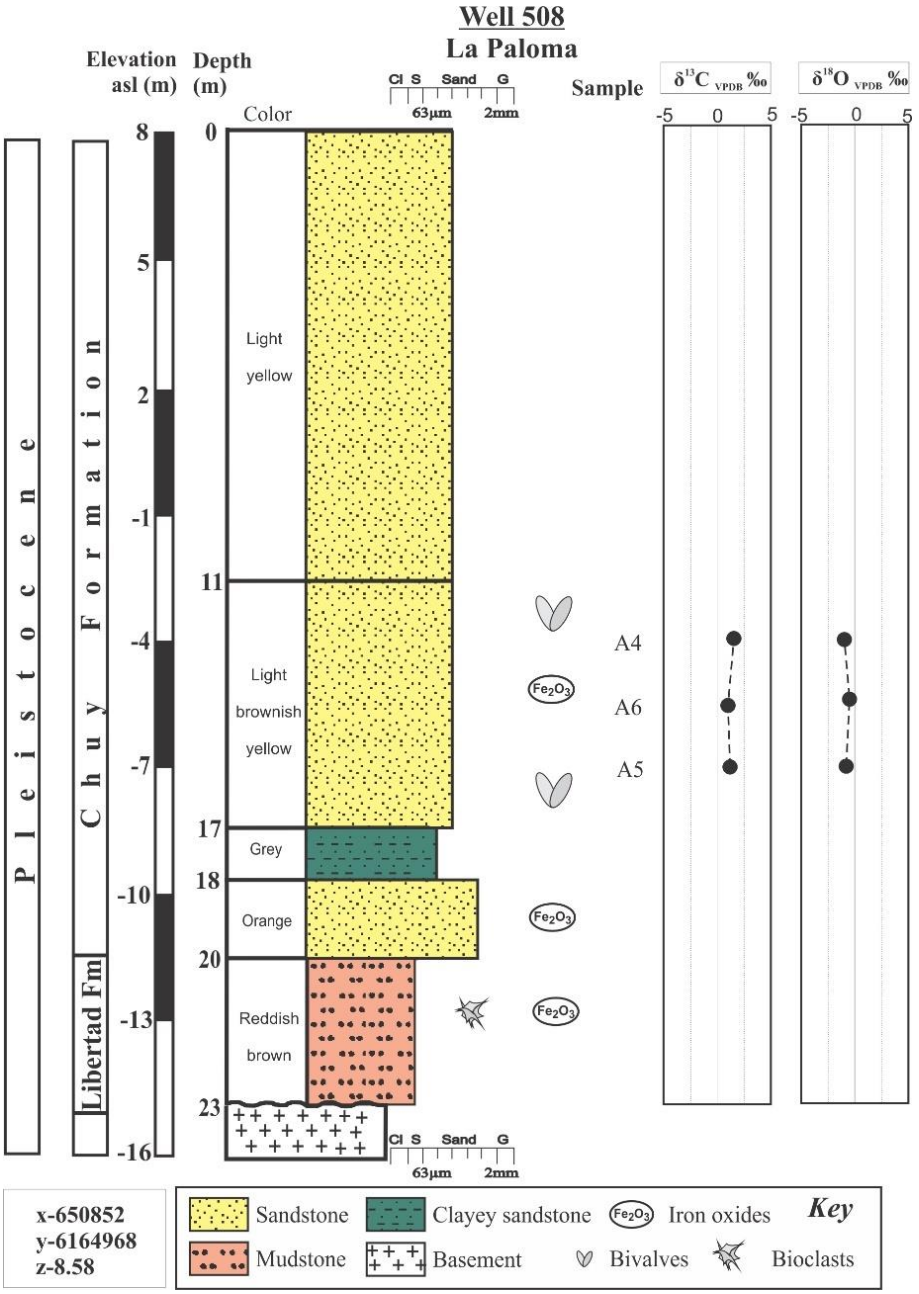

Towards the hinterland (NW) fine sandstones of the Chuy Formation are observed again; they are mainly restricted to a coastal strip between the elevations of 25 and 10 m (Fig. 3), passing to green clays below 10 m of elevation. Towards the center of the La Paloma Graben, a predominance of marine pelitic sediments is observed (Fig. 4). It also presents a marked subsidence characterized by a very insignificant slope with bad drainage, which corresponds to the unit that occupies the largest area in the mapped zone (Fig. 3). Mudstones of the Dolores Formation overlie the Chuy Formation, and lead to the highest elevations in the area, reaching 33 m above MSL.

4.2.2 Libertad Formation

Continental deposits are interdigitated with the marine deposits of the Chuy Formation (Fig. 6), which are assigned to the Libertad Formation *sensu stricto*. These are brownish mudstones with frequent carbonate concretions. Its thickness in outcrops reaches 2.5 m, for example, in the gullies of Santa Isabel (Fig. 6). In the wells described, however, thicknesses of up to 30 m are recorded for continental deposits assignable to the Libertad Formation (Figs. 8, 11).

Recent ^{14}C AMS datings yielded an age of 20 ka for the Libertad Formation in the study area (Antonella Celio, pers. comm., 2019). In well LRO 14 (depth 2.6-2.8 m) an age of 19,030±770 years is reported

(Fig. 5) for an interval of more than 1 m thick of semi-arid continental origin[9], age that coincides, within the error, with the abovementioned. Another similar age 19.5 ka cal BP has been found in the south of Rio Grande do Sul, also in continental sediments[42].

4.2.3 Dolores Formation

In the study area, this Formation occurs along route 10 in the NE part (elevation 25 to 33 m), and between elevations of 10 and 33 m in the SW part. It should be noted that the unit is observed more frequently at the edges of the La Paloma Graben, not occurring in the central part of the basin. The outcrops are scarce and very restricted to erosion gullies, occupying their upper part (Fig. 6).

4.3 ^{14}C Radiochronology

The results of the ^{14}C datings are presented in Table 2, measured as ^{14}C years BP and calibrated[44], for which the reservoir effect of the ocean is contemplated[45]. These dates yielded an uncorrected result of 12,035±110 years for the sample located at -2.75 ± 3 m elevation, 39,995 ±1995 years for the sample located at -6.13 m, and 47,200±2900 years for the sample located at -8 m. It is observed that at greater depth (lower elevation) older ages are recorded. These ages at those elevations for marine mollusks do not coincide with the levels set for the MSL at that time. Paleoshorelines at these ages should be located several tens of meters below the current MSL and hundreds of km to the S of the area, on the current continental shelf. The implications of the data are discussed below. It should be noted that the use of more recent calibration curves[46] yields slightly different calibrated ages (all 1 sigma): for sample E11 of 11970±117 years, for A1 of 41525±1212 years, and for A7 of 47790±2821 years. Since most of the ages available in the literature were calculated with the previous model[45], such calibration is used for ease of comparison.

4.4 Stable isotopes

Table 3 shows the results of analysis of C and O isotopes for samples from the different boreholes studied, expressed in ‰ compared to the international standard VPDB (Vienna Pee Dee Belemnite) and the SMOW (Standard Mean Ocean Water). The marine origin of the invertebrates is confirmed based on their isotopic composition[47] (Fig. 13), as already suggested by paleoecological studies[9][22].

Figure 13. Diagram $\delta^{18}O$ vs. $\delta^{13}C$[47] for the invertebrates analyzed. Note their clear marine origin

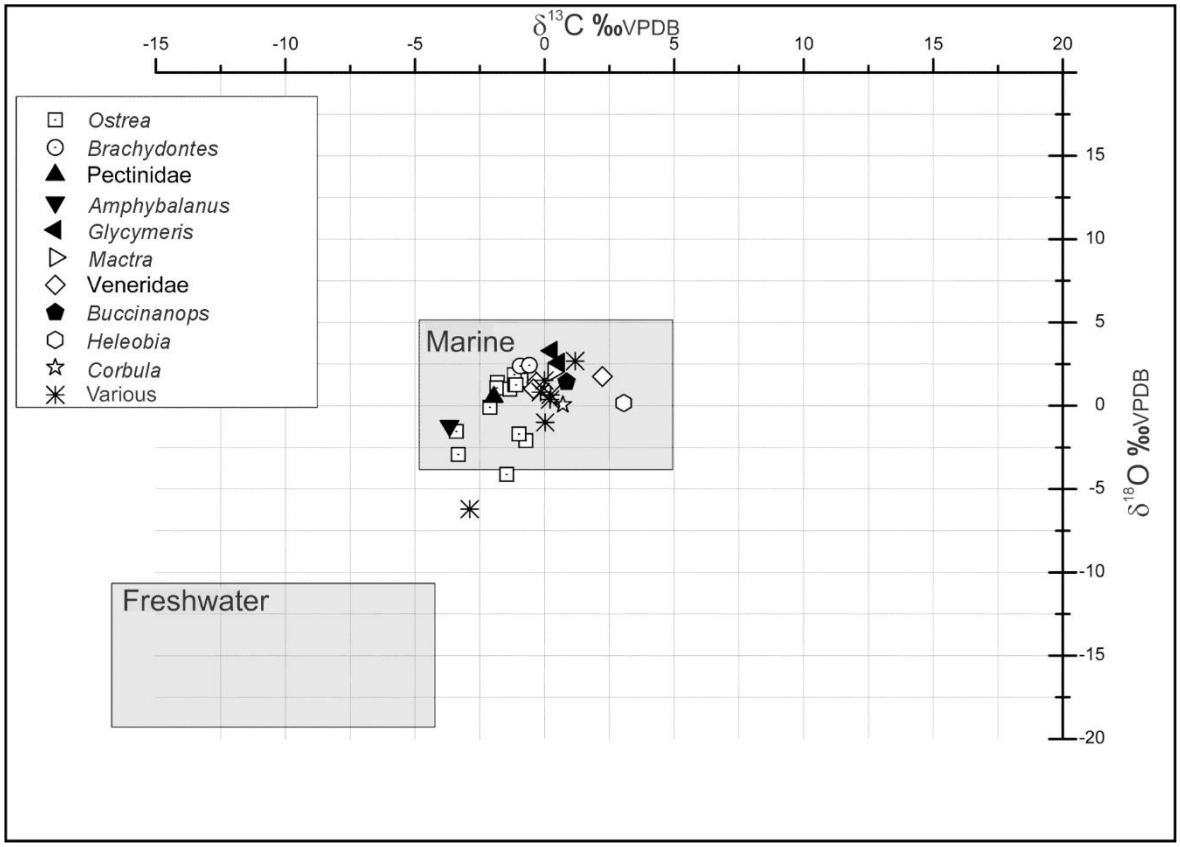

Since the material analyzed corresponds to invertebrate valves (mollusks and crustaceans), the obtained value of $\delta^{18}O$ and $\delta^{13}C$ is generally not equivalent to that of seawater, since there is an isotopic fractionation caused by the metabolism of the organism, known as "vital effect"[48-50]. In order to determine the vital effect of $\delta^{18}O$, a series of valves from present-day specimens of the same species, genera and/or families (as the case may be), like the ones found in the Chuy Formation, were analyzed. The specimens analyzed (Table 4) also come from the Atlantic coast of Uruguay, in areas near La Paloma or from the Chuy Formation type area (well 1257 Barra del Chuy). The vital effect for the invertebrates of interest was calculated using the current value of $\delta^{18}O$ of -0.25 "VSMOW (=-0.45 VPDB) for the waters of the Atlantic coast of Uruguay[51-52] and the corresponding temperature equation[53], which allows finding the equilibrium value of calcite for this isotopic composition of water[54] and the average temperature of 15.1°C. With the values obtained from the vital effect, the correction of the raw values available for all the old samples of the Chuy Formation was carried out (Table 3). The mollusks classified as *Heleobia*, *Veneridae*, *Corbula, Bucinanops* and those marked as "various" were not corrected because no modern specimen information was available, in the case of the former, and because the latter were unidentifiable.

Table 4. Values of $\delta^{18}O$ for current invertebrates and calculated vital correction factor (see text)

Species	Value of $\delta^{18}O_{(VPDB)}$ of the valve	Vital Factor
Brachidontes rodriguezi	-0,14	-0,102
Pectinidae gen, et sp,	-0,09	-0,052
Amphybalanus sp,	-0,14	-0,102
Glycymeris longior	0,00	0,038
Mactra guidoii	1,05	1,088
Ostrea sp.	-1,13	-1,092

For chemo-stratigraphic use, the obtained values of $\delta^{18}O$ (measured and corrected by vital effect) were plotted against the sample elevation, obtaining the curve shown in Figure 14. The points of the curve come from several wells, combining them into a single integrated curve as an input to allow making regional inferences regarding the isotopic oxygen stages (MIS) in which they were deposited[55-56]. It is important to note that the record is not continuous, since there is no record of marine sediments at the time when the Libertad and Dolores Formations were deposited, representing hiatus in the curve of Figure 14.

Figure 14. Curve of oxygen isotope ratio ($\delta^{18}O$) variations relative to elevation for invertebrate samples extracted from the Chuy Formation in the study area and stratotype (Table 3). The position of ^{14}C datings and the interval corresponding to the different marine isotopic stages (MIS) are indicated. Note that around colder intervals (MIS 2, 4 and 6) erosion or continental deposition predominate, therefore, not being fully represented in the curve

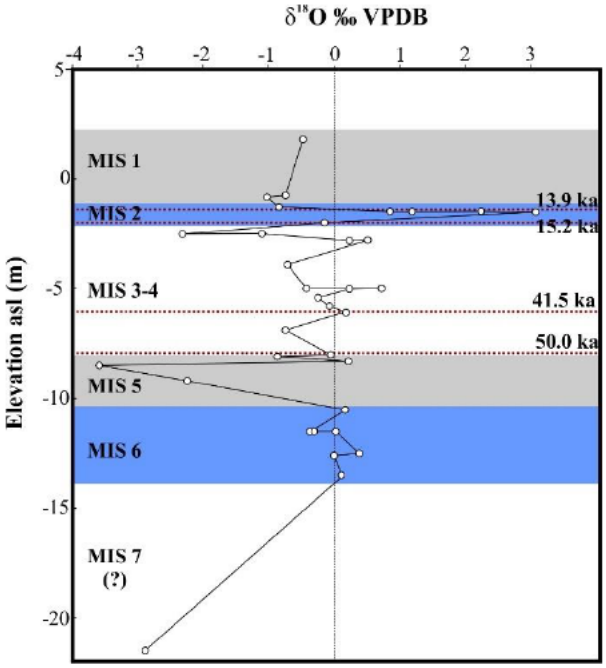

5. Discussion

5.1 Ages and their meaning

The appearance of mollusks of shallow marine origin at the referred elevations (-3 to -8 m), with ages ^{14}C corresponding to the last glaciation, contradicts the general idea that the Chuy Formation was deposited during an interglacial period[18][32]. ^{14}C ages between 35 and 29.5 ka were reported for the Chuy Formation in La Coronilla (Rocha) and Nueva Palmira (Colonia), with maximum levels of 0,6 m for the first case, and up to 13 m for the second[17]. The aforementioned authors interpret that these would be minimum ages and not the age of deposition, which they assign to the last interglacial (115-130 ka, MIS 5e)[56] based on the association of mollusks of warmer temperatures than the current one[57]. An OSL age of 80.7 ka reported

for Nueva Palmira[57] suggests a reset of the ^{14}C ages but does not solve the elevation anomalies. Even if the deposit had occurred in the last interglacial, the elevations recorded in Nueva Palmira would not be explained without isostatic uplifting movements. In the area of Arroyo Chuí (Brazil), immediately at the E of the border with Uruguay, ^{14}C ages of 42 ka were reported in marine mollusks, at elevations of -10 m and, therefore, in a situation similar to those mentioned above[58]. In the same area, a ^{14}C age of 39.6 ka[59], although interpreted as minimum age, was obtained from mollusks in the well Cist-1-RS[31] between 27 and 30 m depth.

The same situation is found in Ezeiza (Province of Buenos Aires, Argentina) with mollusks similar to those of the La Paloma area (*Ostrea puelchana, Mactra isabelleana, Corbula* sp.) at elevation +3.5 m, which yielded ^{14}C ages AMS from 33.7±0.55 ka to 39.9± 1.2 ka, and OSL of 22.1± 1.32 ka[20]. They would correspond to MIS2/3, but the elevations are not consistent with the sea level at that time. On the contrary, other authors obtained similar ^{14}C ages (33.8 to 25.7 ka) in Mar del Sur (Province of Buenos Aires), but interpret them as the real deposit age, indicating that the aragonitic mineralogical composition is preserved and that the values obtained are far from the detection limit of the technique[19]. Similarly, ^{14}C AMS ages of between 36 and 48 ka in southern Brazil were interpreted as depositional ages during MIS 3, and also come from marine deposits at anomalous elevations (-5 to -20 m)[60].

It is clear that either the ages obtained do not represent the age of deposition or if they really represent the depositional age, a subsequent isostatic uplift must be invoked that places the marine sediments at much higher elevations than those of their formation. While it cannot be ruled out, two independent facts suggest that these ages are unlikely to be resetted: (a) the ages were obtained in various materials and with different methods, such as conventional ^{14}C and AMS in mollusks and organic matter[9][58][60], OSL[20] dating and even electron spin resonance (ESR) in mammal teeth[61]. (b) If some post-depositional process is considered to have resetted ^{14}C ages of the Late Pleistocene, the ages of the Holocene marine sediments (<11.7 ka) should also be questioned since the diagenetic conditions they suffered are essentially the same and are only somewhat younger than several of the ages obtained for the Chuy Formation in the study area. However, there is some consensus in interpreting the ^{14}C ages of Holocene marine sediments as depositional ages, even by those who advocate a reset of the Late Pleistocene ^{14}C ages.

An independent test of the meaning of the ^{14}C ages can be obtained from the oxygen isotopic ratios. For the three datings made, a coincidence is verified in the trends of $\delta^{18}O$ obtained in the same well as those of the global curves[56]. Specifically: (a) 50 ka ago the trend of $\delta^{18}O$ is of relative stability to decreasing (Fig. 14), (b) the samples around 41.5 ka indicate a clear increase of $\delta^{18}O$ (Fig. 14), and (c) the samples after the age of 13.9 ka show a constant decrease of $\delta^{18}O$ (Fig. 14), in accordance with what was recorded worldwide during the end of MIS 2[56]. The coincidences found agree with the interpretation of the ^{14}C ages as depositional ages. From the comparison of the integrated curve of $\delta^{18}O$ relative to the elevation for the coast of Rocha, it can be inferred that the studied interval of the Chuy Formation (up to -21.5 m of elevation) covers two glaciations, between the periods MIS 1 to MIS 7 (Fig. 14), although the MIS 7 would only be represented by a sample in well 1060. It is interesting to note that between the elevations of -10 and -45 m there are continental mudstones deposits (Libertad I Formation) in several wells: 733, 1224/1, 482/1, coinciding or immediately below the range of elevations with high ratios of $\delta^{18}O$ assignable to the glaciation corresponding to MIS 6 (130-150 ka)[56]. In addition, these continental deposits in wells 1224/1 and 482/1 are below levels with bioclasts dated at 41.5 and 50 ka, respectively (Figs. 10-11), which is consistent with an age of around 140 ka for continental sedimentites. Another level of younger continental deposits (Libertad II Formation), dated at 19.0 ka[9], occurs at elevations of -3.5 m within Laguna de Rocha, corresponding to the last glacial maximum (MIS 2) recorded in the curve of $\delta^{18}O$ (Fig. 14). It is important to note that plotting the isotopic values against the elevation implies some uncertainty in the vertical scale since the paleorelief of the basin undoubtedly determined that deposits of the same age can be found at different elevations (Fig. 4). As there is no continuous isotopic record in any of the wells, it is necessary to use this criterion as the first preliminary approach, but it is certainly necessary to build a continuous isotopic local curve, by drilling new wells with core recovery.

In samples from the Chuy Formation or correlated units, mollusk species that are outside their current distribution were recorded. Specifically, in La Coronilla, 12 species of mollusks are cited that have their current southern limit about 800 km NE[57] and in

deposits in southern Brazil, there are four species of warmer waters and one of colder waters[59], which is interpreted according to an age corresponding to the MIS 5 stage, contrary to what is indicated by the datings. This paleoecological evidence is important, but the diversity of mollusks and other groups is also dependent on other factors, such as salinity and bathymetry, which also change in the estuarine environment[22]. In general, latitudinal diversity gradients are complex phenomena with multiple causes[62] and also show migrations from the tropics to cold areas not always linked to climatic changes[63]. Finally, it does not seem likely that the levels of the Chuy Formation dated at 15-12 ka are correlative to those where the diversity of mollusks has been studied, as in La Coronilla[57]. As mentioned above, the $\delta^{18}O$ curve obtained in the area of La Paloma suggests that the Chuy Formation covers at least the stages MIS 1 to MIS 7 up to -21.5 m elevation, with a thickness of about 100 m still without isotopic data (Fig. 4). The MIS 5e would therefore be effectively registered in the Chuy Formation in the study area, although at elevations of -9 to -7 m (Fig. 14), significantly lower than those cited in the literature (0.6 m in La Coronilla).

5.2 Age, elevations and isostatic readjustments

The graph in Fig. 15 was made considering the samples analyzed and other previous datings for the region, where the elevation anomaly of up to 113 m verified in the study area (green curve "Elevation anomaly") is observed, implying a rate of uplift of 1 to 7.4 mm/year ("Rate of Uplift" black curve). In the red curve ("rate of uplift variation") the difference in uplift rate between a sample and the previous one in age was plotted, in order to establish the acceleration or deceleration of this uplift rate over time. This allowed showing that the largest uplift was recorded at the end of the Pleistocene, coinciding with the last deglaciation, when the glacio-isostatic rearrangement of the region began, as it lost the weight of the ice caps. It should be noted that during the MIS 3 (25-60 ka) a *plateau* with a rate of uplift (1-2 mm/year) lower than that of the MIS 2-MIS 1 transition is observed (Fig. 15). Small elevation anomalies and mainly of negative sign are also observed in the Holocene, indicating subsidence in the last 6 to 7 ka.

Something similar to what is observed in the Laguna de Rocha was reported for the Chesapeake Bay (USA), where marine sediments that are above sea level today were dated between 67 and 28 ka[6]. The area, like Uruguay, was not covered by ice, being located more than 300 km south of the ice line, but the effects of glacio-hydro isostasy determined the aforementioned elevation anomalies[6]. It should be noted that the rate of uplift measured in Pleistocene deposits is higher in the south than in the north of South America[65], which is compatible with the glacial isostatic model for the east coast of North America[6]. Subsidence is observed in Chesapeake Bay[6], for the Holocene, as well as in the study area.

Figure 15. Illustrative curves of the operating processes in the study area since 50 ka (see Table 5). **(A)** Global sea-level curve[2][23]. **(B)** Elevation anomaly, defined as the current elevation of the sample minus the sea level at the time of deposition. **(C)** Rate of uplift, which is defined as the elevation anomaly divided by the age of the sample. **(D)** Rate of uplift variation compared to the previous sample, calculated as the difference in rate of uplift between a sample and the previous one in age

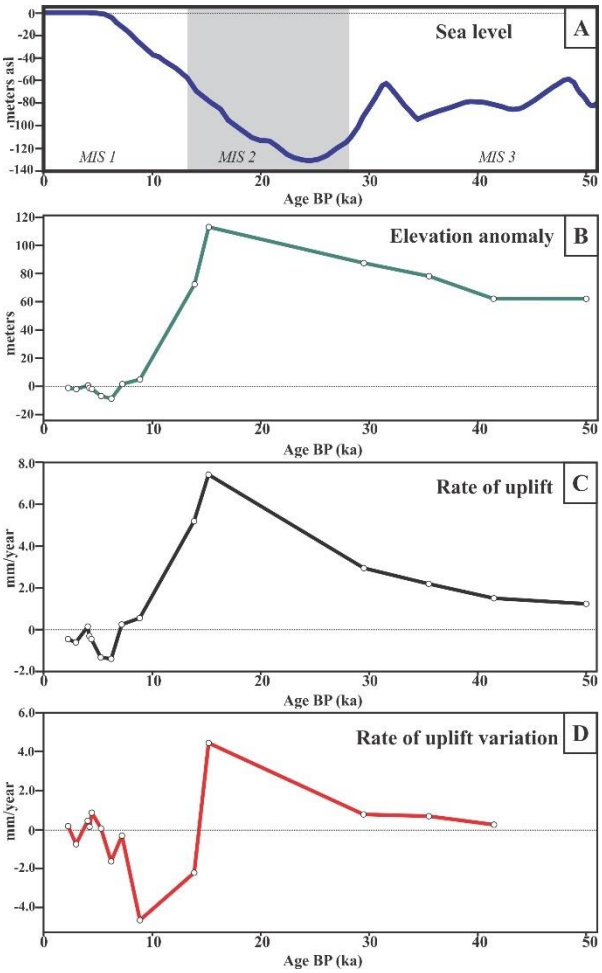

In sediments of the platform in front of Argentina and Uruguay, elevation anomalies were observed that have an opposite sign to those recorded in the samples studied in this research[66-67] (Table 6). In other words, samples of marine mollusks from the Late Pleistocene-Early Holocene on the shelf are at

lower elevations (deeper) than the sea level at the time of deposition. The elevation anomalies, of up to -76 m in Uruguay[67], grow as the distance from the sample to the current coast increases (Table 6). An isostatic uplift on the continent in parallel with isostatic subsidence on the shelf and sea basin is observed in Scandinavia, where rates of uplift of up to 9 mm/year were calculated in the center of the peninsula, 0 mm/year a few km offshore and -2 mm/year in the North Sea[5]. It is clear that the paleogeographic and ice cover situation was very different in both places, but the similar behavior is remarkable, and it is due to a viscoelastic process which pivot point is close to the coast. The opposite sign is explained by the fact that while the continent was covered and depressed by ice, the shelves supported a smaller column of water. When the ice melts, the water column in the shelves increases, causing continent uplift (glacio-isostasy) and platform subsidence (hydro-isostasy, Fig. 16).

Table 5. Ages of samples dated in the region, sea level (relative to present-day msl) is indicated at the time of deposition[2][23] and the elevation anomaly, defined as the current elevation minus the sea level at that time. The sample indicated (*) corresponds to that reported in the expedition of the Meteor research vessel[64], and was located at the base of a core at 144m depth and 91.7 nautical miles (169 km) from the study area. The bathymetry data to which the mollusk found was alive is unknown. Data indicated with (**) correspond to samples from La Coronilla (LP-824 and 884) and Nueva Palmira (LP 730 and 738, not used in Fig. 15), although the authors interpret them as minimum ages[17]. The rate of uplift is defined as the elevation anomaly divided by the age of the sample. In the case of the column "Rate of uplift variation", it refers to the difference in the rate of uplift between a sample and the previous one in age. The ages of the LRO and BOL wells were taken from García-Rodríguez and others[9]

Sample	Age (years BP)	Current elevation (m)	msl (m relative to current msl)	Elevation Anomaly (m)	Rate of uplift (mm/year)	Rate of uplift variation (mm/year)
BOL-1	2250	-1	0	-1	-0.44	-0.17
LRO3-1	2970	-1.3	0.5	-1.8	-0.27	-0.41
LRO12-1	4066	-1.4	-2	0.6	0.14	0.44
LRO3-2	4220	-2.3	-1	-1.3	-0.3	0.14
LRO12-2	4410	-3	-1	-2	-0.44	-0.07
LRO12-3	5269	-5	2	-7	-0.37	-0.12
LRO12-4	6209	-6.6	2	-8.6	-0.25	-0.50
LRO12-5	7207	-7.2	-9	1.8	0.25	-0.30
LRO10	8860	-3.1	-8	4.9	0.55	-4.64
E11	13900	-2.8±3	-75	72.2±3	5.19	-2.21
LRO 14	15187	-2	-115	113	7.4	4.03
LP-884**	29500	0.5	-87	87.5	3.37	0.79
LP-738**	31000	12.5	-80	92.5	2.58	0.27
LP-730**	34600	12.5	-80	92.5	2.31	-0.23
LP-824**	35500	0	-78	78	2.54	1.05
A1	41500	-6.13	-68	61.87	1.49	0.35
A7	50000	-8	-70	62	1.14	--
13802-2*	34600	-144	-75	--	--	--

Table 6. ^{14}C ages and corresponding depths, determined on Pleistocene sediments of the Uruguayan continental shelf in front of the Rocha Department[67]. Sea level at the time of deposition[2], current distance of the sampling point to the coast, and calculated elevation anomaly are indicated

Well	Depth in the well (m)	Depth well opening (m)	Sample elevation (m)	Current sea level (elevation m)	Elevation Anomaly (m)	Distance to coast (km)	^{14}C Age (cal BP)*
13818-4	-2	-40.6	-42.6	-35	-7.6	33	**10.500**
13817-2	-6.5	-61.9	-68.4	-50	-18.4	54	**12.300**
	-10		-71.9	-60	-11.9	54	**13.700**
13815-2	-5	-46.6	-51.6	-30	-21.6	54	**9.900**
13839-1	-4.3	-66.8	-71.1	-40	-31.1	109	**11.000**
13835-2	-4.8	-131.1	-135.9	-60	-75.9	137	**13.200**
13838-2	-1.8	-150.8	-152.5	-110	-42.5	148	**19.500**
	-5		-155.8	-70	-65.8	148	**48.200**

A local behavior hypothesis is proposed in this study, explaining the aforementioned situation[6]. The only plausible mechanism to explain the uplift of about 115 m between approximately 15 and 9 ka is glacio-hydro isostasy, together with eustatic sea level variations. Although Uruguay was ice-free in the last glaciation, it can be a distant effect of glacio-isostatic rebound during the Late Pleistocene. The following steps are recognized in the last 50 ka (Fig. 16):

(a) Between 50 and 41.5 ka the coastline in La Paloma was about 70 m below the current one, implying that the coastal deposits of the Chuy Formation were 62 m below their current level (Fig. 16).

(b) Between 40 and 30 ka the Andean ice sheet grew, generating more subsidence (Fig. 16), which allowed the coastal marine deposition in the studied area to continue at elevations from 78 to 87 m below the current sea level.

(c) Between 20 and 19 ka continental deposits of the Libertad Formation[9] (A. Celio, pers. comm., 2019) are recorded, indicating that the rate of eustatic sea level regression during the last glacial maximum, of about 8 mm/year[68], was higher than the rate of glacial isostatic subsidence. As a result, the coastline retreated to the south, leaving the Laguna de Rocha area in emerged territory (Fig. 16), leading to continentalization.

(d) From 15 to 14 ka, coastal marine deposits are once again recorded in La Paloma, showing that the high rate of sea-level rise at that time, of about 12 mm/year[69], exceeded the post-glacial rate of uplift, calculated here at 5 to 7 mm/year, generating a transgression (Fig. 16).

(e) Continental conditions return around 11-10 ka (Fig. 16), as evidenced by mudstones of the Dolores Formation[18], which overlie the Chuy Formation in the study area. The Dolores Formation may therefore correspond to the climatic event *Younger Dryas*[70]. This event is recorded in South America between 11.4 and 10.2 ka BP[71], marking a period of global cooling.

(f) Between 7 and 5 ka the maximum Holocene marine transgression is recorded up to +4 m elevation[11][14], which coincides in the area of La Paloma with small magnitude subsidence. One way to explain this effect would be through the forebulge collapse, according to the models proposed for the northern hemisphere[4][72]. In the case of Chesapeake Bay, the forebulge collapse makes it possible to explain the present-day subsidence observed (1.7 mm/year) and the fact that they are lowlands[6][73], a characteristic also observed in the Rocha Department.

It is noteworthy that systematic changes are observed in the elevation anomalies of the Pleistocene deposits according to their geographical position. Samples of the Chuy Formation and correlated units dated at 35 ka are found in Nueva Palmira[17] (Table 3) at an elevation of 13 m, in La Coronilla (Rocha) at sea level, and in the south of Rio Grande do Sul (Brazil), 200 km NE from Uruguayan border, 15 m below sea level[60]. This increasing uplift in the W-SW direction is consistent with the hypothesis of a glacial isostatic origin since the rate of uplift is higher in areas previously occupied by thick ice, which would be found in the Patagonian Andes precisely in that direction[74]. In the Brazilian SE (State of Espírito Santo) there are marginal-marine deposits corresponding also to MIS 3 (49.5-29.4 ka BP), with identical elevation anomalies[75]. In this case, the authors explained the elevation anomalies through a tectonic uplift[75]. In the Chuy Formation within the area of study, there is no evidence of such young tectonism capable of explaining uplifts of the order

of tens of meters in a few millenia. A tilt due to Andean tectonics would be consistent with the increasing uplift towards the W that is observed, but it is difficult to reconcile with such a short period of time. It is therefore clear that geological studies should continue in order to elucidate the cause of the elevation anomalies.

Figure 16. Evolution of the coast of La Paloma over the last 50 ka in a approximately W-E transect. The relative size of the arrows indicating isostatic movements (uplift, subsidence) and eustatic changes in sea level (transgression, regression) indicate their relative importance at each time. The behavior of the Andean-Patagonian distal cap for each moment is indicated graphically, as well as the lithostratigraphic units deposited in the area of La Paloma

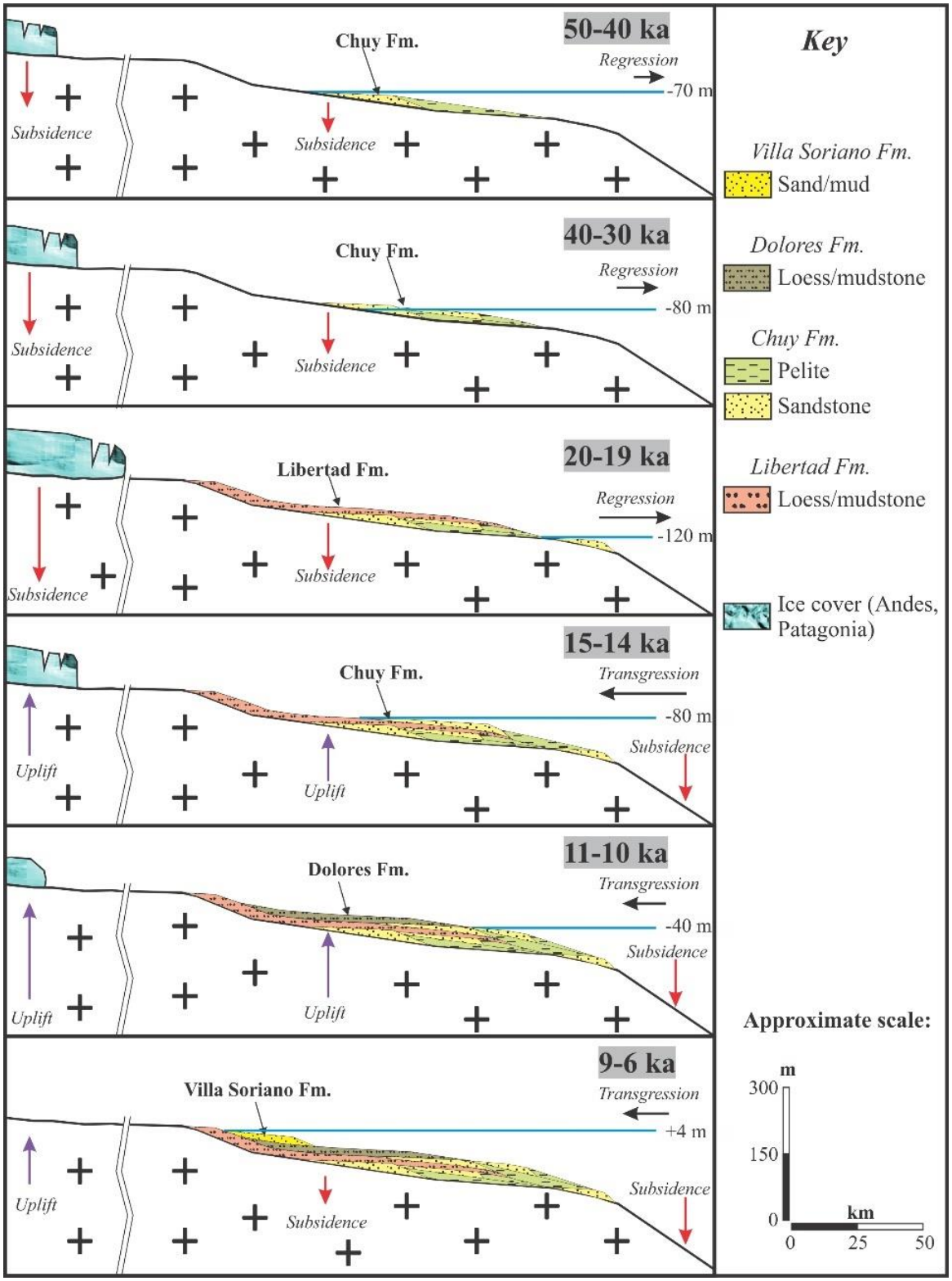

6. Conclusions

The area of La Paloma-Laguna de Rocha is characterized by thick Quaternary deposits that reach their maximum thickness of 140 m in well 1469/1. Most of that thickness corresponds to the Chuy Formation, which is characterized by alternating fine to coarse sandstones and green pelites, with fossils of marine invertebrates. The marine deposits are interbedded with continental loess deposits of the Libertad Formation, and are overlain by the Dolores Formation, also of continental environment.

Radiocarbon dating results showed calibrated ages of 13900±200, 41500±1900 and 50000±3000 cal years BP (using the curve[46], the calibrated ages are: 11970±117, 41525±1212 and 47790±2821 cal years BP), for marine fossil bioclasts at an elevation above mean sea level (amsl) of -2.8, -6.1 and -8 m, respectively. These results agree with ages obtained in cores inside the Laguna de Rocha[9], with 15.2 ka for marine sediments (elevation -2 m) and 19 ka for continental deposits at an elevation of -3.5 m (Libertad Formation).

These ages and elevations, and others from the Chuy Formation reported in the literature, are at odds with the sea level evolution accepted for the Late Pleistocene. It is considered in this study that the most plausible explanation is that radiocarbon ages represent real depositional ages, and therefore, the area must have experienced significant isostatic readjustments during and after the last glaciation. Other evidence favors a Late Pleistocene age for the Upper Chuy Formation, including the $\delta^{18}O$ curve obtained for invertebrate shells, which shows secular isotopic variations consistent with MIS 1 to MIS 7 stages up to -21.5 m elevation.

An alternative explanation considers that the ^{14}C ages for the Chuy Formation are apparent, lower than the real ones and that the unit was deposited during the last interglacial (MIS 5e stage 115-130 ka). The occurrence of some species typical of waters warmer than present-day temperatures, main argument in favor of an MIS 5e age for the Chuy Formation[17][57][59], presents some complexities, given that biodiversity in an estuarine environment is controlled by salinity and bathymetry, in addition to temperature[22]. It is also unlikely that the youngest samples of the Chuy Formation, around 14-15 ka, can be correlated with those localities that present warmer water species. The $\delta^{18}O$ curve reported here for the formation actually shows that MIS 5e may occur at elevations of -9 to -7 m, significantly lower than those cited in the literature (0.6 m in La Coronilla).

The proposed scenario involves subsidence of between 60 and 87 m between 50-20 ka due to the distant effects of the glacial load in the Andes/Patagonia. At 20 ka, eustatic sea-level regression outpaced isostatic subsidence in the Laguna de Rocha area, leading to continentalization. Marine conditions returned at 15 ka and in the Holocene with postglacial transgression, separated by continental deposits (Dolores Formation) at 11-10 ka (*Younger Dryas*). Isostatic uplift of about 115 m occurred between 14 and 9 ka in the area, which is interpreted as a postglacial rebound. Later in the Holocene, moderate subsidence is recorded that may be due to the collapse of the glacial forebulge. Regionally, a trend is observed with an increase in the elevation of Pleistocene marine deposits towards the W-SW, which is consistent with a postglacial isostatic rebound due to the melting of the Andean/Patagonian ice cap. It should be noted that, on the continental shelf, isostatic movements of opposite sign are recorded[66], with increasing hydro-isostatic subsidence the greater the distance to the coast.

Acknowledgments

Prof. Jorge Bossi (*in memoriam*) provided valuable discussions and ideas on the geology of the area of La Paloma, some of which he reflected in his pioneer books "*Geología del Uruguay*". Likewise, Peter Sprechmann (*in memoriam*) provided bibliography and detailed knowledge of the Chuy Formation and the area of study, where he made his now classical doctoral thesis.

The authors thank Jorge Montaño and Sergio Gagliardi for their important contributions to the cartography. Fabrizio Scarabino (CURE) assisted in the identification of mollusks and provided recent material. We thank DINAMIGE for allowing access to the studied boreholes. The suggestions and comments of two anonymous reviewers allowed us to improve the original manuscript; to them, the recognition for their work. The Geosciences Area of PEDECIBA contributed with funds granted to CG.

Author contribution statement

EC carried out field work, collected the data, contributed to data analysis, and wrote the paper. CG conceived and designed the analysis, carried out field work, contributed to data analysis, and wrote the paper. GMEP carried out field work, contributed to data analysis and interpretation, and performed manuscript revision. ANS contributed with

analysis tools, performed the analysis, and performed manuscript revision.

References

1. Petit JR, Jouzel J, Raynaud D, Barkov NI, Barnola JM, Basile I, Bender M, Chappellaz J, Davis M, Delaygue G, Delmotte M, Kotlyakov VM, Legrand M, Lipenkov VY, Lorius C, Pépin L, Ritz C, Saltzman E, Stievenard M. Climate and atmospheric history of the past 420,000 years from the Vostok ice core, Antarctica. Nature. 1999;399:429-36.

2. Waelbroeck C, Labeyrie L, Duplessy EM, McManus JC, Lambeck FK, Balbona E, Labracherie M. Sea-level and deep water temperature changes derived from benthic foraminifera isotopic records. Quat Sci Rev. 2002;21:295-305

3. Chappell J, Shackleton NJ. Oxygen isotopes and sea level. Nature. 1986;324:137-40.

4. Fjeldskaar W. The amplitude and decay of the glacial forebulge in Fennoscandia. Nor J Geol. 1994;74:2-8.

5. Fjeldskaar W, Lindholm C, Dehls JF, Fjeldskaar I. Postglacial uplift, neotectonics and seismicity in Fennoscandia. Quat Sci Rev. 2000;19:1413-22.

6. DeJong BD, Bierman PR, Newell WL, Rittenour TM, Mahan SA, Balco G, Rood DH. Pleistocene relative sea levels in the Chesapeake Bay region and their implications for the next century. GSA Today. 2015;25(8):4-10.

7. Bracco R, Ures C. Las variaciones del mar y el desarrollo de las culturas prehistóricas del Uruguay. In: Actas II Congreso Uruguayo de Geología; 1998 May 13-18, Punta del Este, Uruguay. Montevideo: Facultad de Ciencias; 1998. p. 16-28.

8. García-Rodríguez F, Witkowski A. Inferring sea level variation from relative percentages of *Pseudopodosira kosugii* in Rocha lagoon, SE Uruguay. Diatom Res. 2003;18:49-59.

9. García-Rodríguez F, Metzeltin D, Sprechmann P, Trettin R, Stams G, Beltrán-Morales LF. Upper Pleistocene and Holocene paleosalinity and trophic state changes in relation to sea level variation in Rocha Lagoon, southern Uruguay. J Paleolimnol. 2004;32:117-35.

10. Inda H, García-Rodríguez F, del Puerto L, Acevedo V, Metzeltin D, Castiñeira C, Bracco R, Adams JB. Relationships between trophic state, paleosalinity and climatic changes during the first Holocene marine transgression in Rocha Lagoon, southern Uruguay. J Paleolimnol. 2006;35:699-713.

11. Bracco R, García-Rodríguez F, Inda H, del Puerto L, Castiñeira C, Panario D. Niveles relativos del mar durante el Pleistoceno final – Holoceno y las costas de Uruguay. In: García-Rodríguez F, editor. El Holoceno en la zona costera del Uruguay. Montevideo: Facultad de Ciencias; 2011. p. 65-92.

12. Bossi J, Ortiz A. Geología del Holoceno. In: García-Rodríguez F, editor. El Holoceno en la zona costera del Uruguay. Montevideo: Facultad de Ciencias; 2011. p. 13–48.

13. Martínez S, Rojas A. Relative sea level during the Holocene in Uruguay. Palaeogeogr Palaeoclimatol Palaeoecol. 2013;374:123-31.

14. Angulo RJ, Lessa GC, de Souza MC. A critical review of mid-to late-Holocene sea-level fluctuations on the eastern Brazilian coastline. Quat Sci Rev. 2006;25:486-506.

15. Barboza EG, Dillenburg SR, do Nascimento Ritter M, Angulo RJ, da Silva AB, Rosa MLCC, Caron F, de Souza MC. Holocene sea-level changes in southern Brazil based on high-resolution radar stratigraphy. Geosciences [Internet]. 2021 [cited 2022 Mar 31];11: 326. doi:10.3390/geosciences11080326.

16. Goso H. El Cenozoico en el Uruguay. Montevideo: Instituto Geológico del Uruguay; 1965. 36p.

17. Martínez S, Ubilla M, Verde M, Perea D, Rojas A, Guérèquiz R, Piñeiro G. Paleoecology and geochronology of Uruguayan coastal marine Pleistocene deposits. Quat Res. 2001;55:246-54.

18. Ubilla M, Martínez S. Geology and paleontology of the quaternary of Uruguay. New York: Springer; 2016. 77p.

19. Tonni EP, Carbonari JE, Huarte R. Marine sediments attributed to marine isotope stage 3 in the southeastern Buenos Aires province, Argentina. Current Research in the Pleistocene. 2010;27:154-6.

20. Martinez S, del Río CJ, Rojas A. A Pleistocene (MIS 5e) mollusk assemblage from Ezeiza (Buenos Aires Province, Argentina). J S Am Earth Sci. 2016;70:174-87.

21. Gómez EA, Perillo GME. Sediment outcrops underneath shoreface-connected sand ridges, outer Bahía Blanca estuary, Argentina. Quaternary of South America and Antarctica Peninsula. 1995;9:27-42.

22. Sprechmann P. The paleoecology and paleogeography of the Uruguayan coastal area during the Neogene and Quaternary. Zitteliana. 1978;4:3-72.

23. Thompson WG, Goldstein SL. A radiometric calibration of the SPECMAP timescale. Quat Sci Rev. 2006;25:3207-15.

24. Bossi J, Ferrando L, Montaña J, Campal N, Morales H, Gancio F, Schipilov A, Piñeyro D, Sprechmann P. Carta geológica del Uruguay: escala 1:500.000. Montevideo: Geoeditores; 1998. 145p.

25. Abre P, Blanco G, Gaucher C, Frei D, Frei R. Provenance of the Late Ediacaran Rocha Formation, Cuchilla Dionisio Terrane, Uruguay: tectonic implications on the assembly of Gondwana. Precambrian Res [Internet]. 2020 [cited 2022 Mar 31];342:105704. doi:10.1016/j.precamres.2020.105704.

26. Blanco G, Abre P, Cabrera J, Gaucher C. Formación Rocha. In: Bossi J, Gaucher C, editors. Geología del Uruguay. Vol. 1, Predevónico. Montevideo: Polo; 2014. p. 401-8.

27. Bossi J, Gaucher C. The Cuchilla Dionisio Terrane, Uruguay: an allochthonous block accreted in the Cambrian to SW-Gondwana. Gondwana Res. 2004;7:661-74.

28. Bossi J, Schipilov A. Rocas ígneas básicas del Uruguay. Montevideo: Facultad de Agronomía; 2007. 363p.

29. Cernuschi F, Dilles JH, Kent AJR, Schroer G, Raab AK, Conti B, Muzio R. Geology, geochemistry and geochronology of the Cretaceous Lascano East Intrusive Complex and magmatic evolution of the Laguna Merín Basin, Uruguay. Gondwana Res. 2015;28:837-57.

30. Machado JPSL, Jelinek AR, Stephenson R, Gaucher C, Bicca MM, Chiglino L, Genezini FA. Low-temperature thermochronology of the South Atlantic margin along Uruguay and its relation to tectonic events in West Gondwana. Tectonophysics [Internet]. 2020 [cited 2022 Mar 31];784:228439. doi:10.1016/j.tecto.2020.228439.

31. Closs D. Estratigrafia da Bacia de Pelotas, Rio Grande do Sul. Iheringia Sér Geol. 1970;3:3-76.

32. Bossi J, Navarro R. Geología del Uruguay. Montevideo: Universidad de la República; 1991. 2v.

33. Fariña RA, Tambusso PS, Varela L, Czerwonogora A, Di Giacomo M, Musso M, Bracco R, Gascue A. Arroyo del Vizcaíno, Uruguay: a fossil-rich 30-ka-old megafaunal locality with cut-marked bones. Proc Biol Sci [Internet]. 2013 [cited 2022 Mar 31];281(1774):20132211. doi:10.1098/rspb.2013.2211.

34. Delaney PJV. Quaternary geologic history of the coastal plain of Rio Grande do Sul, Brasil. Baton Rouge: Louisiana State University Press; 1963. 63p.

35. Goñi JC, Hoffstetter R. Uruguay. In: Hoffstetter R, editor. Lexique stratigraphique international, Fascicule 9-a. Paris: Centre National de la Recherche Scientifique; 1964. p. 1-202.

36. Elizalde G. Conservación y mejora de playas. Montevideo: UNESCO; 1976. 12p.

37. Bossi J, Ferrando LA, Fernández A, Elizalde G, Morales H, Ledesma J, Carballo E, Medina E, Ford I, Montaña J. Carta geológica del Uruguay: escala 1/1.000.000. Montevideo: MAP; 1975. 32p.

38. Goso H, Anton D. Estado actual de los conocimientos sobre el Cuaternario en el Uruguay. In: Anais do XXVIII Congresso Brasileiro de Geologia; 1974; Porto Alegre. São Paulo: Sociedade Brasileira de Geologia; 1974. p. 1-7.

39. Goso H. Cuaternario: programa de estudio y levantamiento de suelos. Montevideo: MGAP; 1972. 12p.

40. Bossi J, Ferrando L. Carta Geológica del Uruguay: escala 1/500.000 versión digital. Montevideo: Facultad de Agronomía; 2001. 1 CD-ROM.

41. Craig H. Isotopic standards of carbon and oxygen and correction factors for mass-spectrometric analysis of carbon dioxide. Geochim Cosmochim Acta. 1957;12:133-49.

42. Rosa MLCDC, Barboza EG, Abreu VDS, Tomazelli LJ, Dillenburg SR. High-frequency sequences in the quaternary of Pelotas Basin (coastal plain): a record of degradational stacking as a function of longer-term base-level fall. Braz J Geol. 2017;47:183-207.

43. Castiglioni EA. Variaciones del nivel del mar, glacio- e hidroisostáticas en la Laguna de Rocha y zonas aledañas, Uruguay [doctoral's thesis]. Bahía Blanca (AR): Universidad Nacional del Sur; 2020. 227p.

44. Blackwell PG, Buck CE, Reimer PJ. Important features of the new radiocarbon calibration curves Quat Sci Rev. 2005;25:408-13.

45. Hughen KA, Baillie MGL, Bard E, Warren Beck J, Bertrand CJH, Blackwell PG, Buck CE, Burr GS, Cutler KB, Damon PE, Edwards RL, Fairbanks RG, Friedrich M, Guilderson TP, Kromer B, McCormac G, Manning S, Bronk Ramsey C, Reimer PJ, Reimer RW, Remmele S, Southon JR, Stuiver M, Talamo S, Taylor FW, VAN der Plicht J, Weyhenmeyer CE. Marine04 marine radiocarbon age calibration, 0–26 Cal Kyr Bp. Radiocarbon. 2004;46(3):1059–86.

46. Reimer PJ. Composition and consequences of the IntCal20 radiocarbon calibration curve. Quaternary Res. 2020;96:22-7.

47. Keith ML, Weber JN. Carbon and Oxigen isotopic composition of selected limestones and fossils. Geochim Cosmochim Acta. 1964;28:1787-16.

48. Weber JN, Woodhead PMJ. Temperature dependance of oxygen-18 concentration in reef coral carbonates. J Geophys Res. 1972;77:463-73.

49. Hoefs J. Stable isotope geochemistry. Berlin: Springer; 1997. 201p.

50. Adkins JF, Boyle EA, Curry WB, Lutringer A. Stable isotopes in deep-sea corals and a new mechanism for vital effects. Geochim Cosmochim Acta. 2002;67:1129-43.

51. Schmidt GA, Bigg GR, Rohling EJ. Global Seawater Oxygen-18 Database [Internet]. v1.22. [place unknown]: NASA; 1999 [cited 2022 Mar 31]. Available from: https://data.giss.nasa.gov/o18data/.

52. LeGrande AN, Schmidt GA. Global gridded data set of the oxygen isotopic composition in seawater. Geophys Res Lett [Internet]. 2006 [cited 2022 mar 31];33:12604. doi:10.1029/2006GL026011.

53. O'Neil JR, Clayton RN, Mayeda TK. Oxygen isotope fractionation in divalent metal carbonates. J Chem Phys. 1969;51:5547-58.

54. Pados T, Spielhagen RF, Bauch D, Meyer H, Segl M. Oxygen and carbon isotope composition of modern planktic foraminifera and near-surface waters in the Fram Strait (Arctic Ocean): a case study. Biogeosciences. 2015;12:1733-52.

55. Lisiecki LE, Raymo ME. A Pliocene-Pleistocene stack of 57 globally distributed benthic δ18O records. Paleoceanography. 2005;20:1-17.

56. Lisiecki LE, Raymo ME. Diachronous benthic $\delta^{18}O$ responses during late Pleistocene terminations. Paleoceanography [Internet]. 2009 [cited 2022 Mar 31];24:PA3210. doi:10.1029/2009PA001732.

57. Rojas A, Martínez S. Marine Isotope Stage 3 (MIS 3) Versus Marine Isotope Stage 5 (MIS 5) Fossiliferous Marine Deposits from Uruguay. In: Gasparini GM, Rabassa J, Deschamps C, Tonni EP, editors. Marine Isotope Stage 3 in Southern South America, 60 KA BP-30 KA BP. Cham: Springer; 2016. p. 249-78.

58. Lima LG, Dillenburg SR, Medeanic S, Barboza EG, Rosa MLC, Tomazelli LJ, Dehnhardt BA, Caron F. Sea-level rise and sediment budget controlling the evolution of a transgressive barrier in southern Brazil. J S Am Earth Sci. 2013;42:27-38.

59. Martínez S, Coimbra JC, Rojas A. Last Interglacial mollusks from the subsurface of the Rio Grande do Sul Coastal Plain, southernmost Brazil. J S Am Earth Sci [Internet]. 2019 [cited 2022 Mar 31];96:102331. doi:10.1016/j.jsames.2019.102331.

60. Dillenburg SR, Barboza EG, Rosa MLC, Caron F, Cancelli R, Santos-Fischer CB, Lopes RP, do Nascimento Ritter M. Sedimentary records of marine isotopic stage 3 (MIS 3) in southern Brazil. Geo-Mar Lett. 2019;40:1099-108.

61. Lopes RP, Oliveira LC, Figueiredo AMG, Kinoshita A, Baffa O, Buchmann FS. ESR dating of Pleistocene mammal teeth and its implications for the biostratigraphy and geological evolution of the coastal plain, Rio Grande do Sul, southern Brazil. Quat Int. 2010;212:213-22.

62. Willig MR, Kaufman DM, Stevens RD. Latitudinal gradients of biodiversity: pattern, process, scale, and synthesis. Annu Rev Ecol Evol Syst. 2003;34:273-309.

63. Jablonski D, Roy K, Valentine JW. Out of the tropics: evolutionary dynamics of the latitudinal diversity gradient. Science. 2006;314:102-6.

64. Klicpera A. Carbonate secreting organisms in clastic shelf systems and their potential as environment archive [doctoral's thesis]. Bremen (DE): Universität Bremen; 2014. 199p.

65. Rostami K, Peltier WR, Mangini A. Quaternary marine terraces, sea-level changes and uplift history of Patagonia, Argentina: comparisons with predictions of the ICE-4G (VM2) model of the global process of glacial isostatic adjustment. Quat Sci Rev. 2000;19:1495-525.

66. Guilderson TP, Burckle L, Hemming S, Peltier WR. Late Pleistocene sea level variations derived from the Argentine Shelf. Geochemistry Geophys Geosystems [Internet]. 2000 [cited 2022 Mar 31];1(12). doi:10.1029/2000GC000098.

67. Lantzsch H, Hanebuth TJ, Chiessi CM, Schwenk T, Violante RA. The high-supply, current-dominated continental margin of southeastern South America during the late Quaternary. Quat Res. 2014;81:339-54.

68. Lambeck K, Rouby H, Purcell A, Sun Y, Sambridge M. Sea level and global ice volumes from the Last Glacial Maximum to the Holocene. Proc Natl Acad Sci U S A. 2014;111:15296-303.

69. Bard E, Hamelin B, Delanghe-Sabatier D. Deglacial meltwater pulse 1B and Younger Dryas sea levels revisited with boreholes at Tahiti. Science. 2010;327:1235-7.

70. Fairbanks RG. A 17,000-year glacio-eustatic sea level record: influence of glacial melting rates on the Younger Dryas event and deep ocean circulation. Nature. 1989;342:637-42.

71. Hajdas I, Bonani G, Moreno PI, Ariztegui D. Precise radiocarbon dating of Late-Glacial cooling in mid-latitude South America. Quat Res. 2003;59:70-8.

72. Wickert AD, Anderson RS, Mitrovica JX, Naylor S, Carson EC. The Mississippi River records glacial-isostatic deformation of North America. Sci Adv [Internet]. 2019 [cited 2022 Mar 31];5(1):eaav2366. doi:10.1126/sciadv.aav2366.

73. Scott TW, Swift DJ, Whittecar GR, Brook GA. Glacioisostatic influences on Virginia's late Pleistocene coastal plain deposits. Geomorphology. 2010;116:175-88.

74. Davies BJ, Darvill CM, Lovell H, Bendle JM, Dowdeswell JA, Fabel D, Garcia J-L, Geiger A, Glasser NF, Gheorghiu DM, Harrison S, Hein AS, Kaplan MR, Martin JRV, Mendelova M, Palmer A, Pelto M, Rodes A, Sagredo EA, Smedley RK, Smellie JL, Thorndycraft VR. The evolution of the Patagonian Ice Sheet from 35 ka to the present day (PATICE). Earth Sci Rev [Internet]. 2020 [cited 2022 Mar 31];204:103152. doi:10.1016/j.earscirev.2020.103152.

75. Cohen MCL, França MC, de Fátima Rossetti D, Pessenda LCR, Giannini PCF, Lorente FL, Buso Jr AA, Castro D, Macario K. Landscape evolution during the late Quaternary at the Doce River mouth, Espírito Santo State, southeastern Brazil. Palaeogeogr Palaeoclimatol Palaeoecol. 2014;415:48-58.